ปฏิกิริยาไฮโดรจิเนชันแบบเลือกเกิดได้ของสามไนโตรสไตรรีนไปเป็นสามไวนิลอะนิลีน
บนตัวเร่งปฏิกิริยาไบเมทัลลิคที่มีแพลตินัมเป็นองค์ประกอบหลัก

นายสถาพร เทียนเสริมทรัพย์

วิทยานิพนธ์นี้เป็นส่วนหนึ่งของการศึกษาตามหลักสูตรปริญญาวิศวกรรมศาสตรมหาบัณฑิต
สาขาวิชาวิศวกรรมเคมี ภาควิชาวิศวกรรมเคมี
คณะวิศวกรรมศาสตร์ จุฬาลงกรณ์มหาวิทยาลัย
ปีการศึกษา 2559

SELECTIVE HYDROGENATION OF 3-NITROSTYRENE TO 3-VINYLANILINE OVER PT-BASED BIMETALLIC CATALYSTS

Mr. Sathaporn Tiensermsub

A Thesis Submitted in Partial Fulfillment of the Requirements
for the Degree of Master of Engineering Program in Chemical Engineering
Department of Chemical Engineering
Faculty of Engineering
Chulalongkorn University
Academic Year 2016

Thesis Title	SELECTIVE HYDROGENATION OF 3-NITROSTYRENE TO 3-VINYLANILINE OVER PT-BASED BIMETALLIC CATALYSTS
By	Mr. Sathaporn Tiensermsub
Field of Study	Chemical Engineering
Thesis Advisor	Associate Professor Joongjai Panpranot, Ph.D.

Accepted by the Faculty of Engineering, Chulalongkorn University in Partial Fulfillment of the Requirements for the Master's Degree

.....Dean of the Faculty of Engineering

(Associate Professor Supot Teachavorasinskun, D.Eng.)

THESIS COMMITTEE

.....Chairman

(Professor Bunjerd Jongsomjit, Ph.D.)

.....Thesis Advisor

(Associate Professor Joongjai Panpranot, Ph.D.)

.....Examiner

(Associate Professor Anongnat Somwangthanaroj, Ph.D.)

.....External Examiner

(Assistant Professor Okorn Mekasuwandumrong, Ph.D.)

สถาพร เทียนเสริมทรัพย์ : ปฏิกิริยาไฮโดรจิเนชันแบบเลือกเกิดได้ของสามไนโตรสไตรรีนไปเป็นสามไวนิลอะนิลีนบนตัวเร่งปฏิกิริยาไบเมทัลลิคที่มีแพลตินัมเป็นองค์ประกอบหลัก (SELECTIVE HYDROGENATION OF 3-NITROSTYRENE TO 3-VINYLANILINE OVER PT-BASED BIMETALLIC CATALYSTS) อ.ที่ปรึกษาวิทยานิพนธ์หลัก: รศ.ดร. จูงใจ ปั้นประณต, 58 หน้า.

เตรียมตัวเร่งปฏิกิริยาไบเมทัลลิคที่มีแพลตินัม0.5% โดยน้ำหนักเป็นองค์ประกอบหลักบนไทเทเนียมไดออกไซด์(P-25) ด้วยวิธีเคลือบฝังร่วมกับโลหะจากแถวที่ 4 ในตารางธาตุได้แก่ โครเมียม เหล็ก โคบอลต์ นิกเกิล ทองแดง สังกะสี และ แกลเลียม ทดสอบความว่องไวของตัวเร่งปฏิกิริยาที่เตรียมขึ้นในปฏิกิริยาไฮโดรจิเนชันแบบเลือกเกิดได้ของสามไนโตรสไตรีนไปเป็นสามไวนิลอะนิลีนในวัฏภาคของเหลวภายใต้ความดันไฮโดรเจน 2 เมกะปาสคาลและอุณหภูมิ 50 องศาเซลเซียล พบว่าชุดตัวเร่งปฏิกริยาแพลตินัม-เหล็กที่ปริมาณเหล็ก 0.2-0.7% โดยน้ำหนักให้ค่าคอนเวอร์ชันของไนโตรสไตรีนและการเลือกเกิดเป็นไวนิลอะนิลีนสูงกว่าตัวเร่งปฏิกริยาที่มีเพียงโลหะแพลตินัม ส่วนการเติมโคบอลต์(0.3-0.5%) และแกลเลียม(0.2-0.5%) ให้ผลที่ดีเช่นเดียวกัน ความว่องไวของตัวเร่งปฏิกริยาไม่สอดคล้องกับปริมาณการดูดซับของแก๊สคาร์บอนมอนอกไซด์อาจเนื่องมาจากการเกิดอัลลอยของโลหะผสมแพลตินัมและการบดบังของตำแหน่งของแพลตินัมที่ว่องไว อย่างไรก็ตามจากเทคนิคการรีดักชันแบบโปรแกรมอุณหภูมิการเติมโลหะตัวที่สอง ช่วยส่งเสริมการรีดิวซ์ของโลหะแพลตินัมทำให้อุณหภูมิรีดักชันต่ำลง และการกระเจิงรังสีเอ็กซ์ แสดงการเกิดโครงสร้างอสัณฐานปกคลุมตัวเร่งปฏิกริยาซึ่งช่วยเพิ่มค่าการเลือกเกิดเป็นไวนิลอะนิลีน ตัวเร่งปฏิกิริยาที่ดีที่สุดคือตัวเร่งปฏิกิริยา 0.5 แพลตินัม-0.5เหล็กบนตัวรองรับไทเทเนีย โดยให้ปริมาณผลิตภัณฑ์ที่ไม่ต้องการต่ำที่สุดประมาณ 0.2 เปอร์เซ็นต์ ในขณะที่ให้ค่าร้อยละผลได้ ของไวนิลอะนิลีนสูงที่สุดที่ร้อยละ 78

ภาควิชา วิศวกรรมเคมี ลายมือชื่อนิสิต .....

สาขาวิชา วิศวกรรมเคมี ลายมือชื่อ อ.ที่ปรึกษาหลัก .....

ปีการศึกษา 2559

5670416921 : MAJOR CHEMICAL ENGINEERING

KEYWORDS: 3-NITROSTYRENE HYDROGENATION / CO-IMPREGNATION / PLATINUM CATALYST / BIMETALLIC

SATHAPORN TIENSERMSUB: SELECTIVE HYDROGENATION OF 3-NITROSTYRENE TO 3-VINYLANILINE OVER PT-BASED BIMETALLIC CATALYSTS. ADVISOR: ASSOC. PROF. JOONGJAI PANPRANOT, Ph.D., 58 pp.

The Pt-based bimetallic catalysts on degussa P25 titanium dioxide were synthesized by co-impregnation method with metal from the 4th row of periodic table such as Cr, Fe, Co, Ni, Cu, Zn, and Ga. The catalytic activities were tested in the liquid-phase selective hydrogenation of 3-nitrostyrene (3-NS) to 3-vinylaniline (3-VA) under 2 MPa of H_2 and 50ºC. I was found that the 0.5Pt-xFe/TiO_2 series exhibited superior NS conversion and higher 3-VA selectivity than the monometallic Pt catalyst. The Pt-Co(0.3-0.5%) and Pt-Ga(0.2-0.5%) also showed improved catalytic performances. The activity of the bimetallic Pt-based catalysts did not follow the CO-chemisorption trend due probably to the Pt-alloy formation and/or the coverage of Pt active site by the 2nd metal. However, the H_2-TPR results showed that the reducibility of Pt oxide was easier for the bimetallic catalysts and the XRD results revealed the presence of amorphous phase when Fe, Co, or Ga were added to the Pt catalysts. This could be the reason for higher VA selectivity of these catalysts. The 0.5Pt-0.5Fe/TiO_2 showed the best catalytic performances which gave the lowest undesire product (3-ethylnitrobenzene) about 0.2 % with the highest yield of 3-VA at 78%.

Department: Chemical Engineering Student's Signature .....

Field of Study: Chemical Engineering Advisor's Signature .....

Academic Year: 2016

ACKNOWLEDGEMENTS

The author is grateful to Associate Professor Joongjai Panpranot for her advice, suggestion, knowledge, and continuous diccussion. I really appreciated her thought time during this research.

In addition, the author also would like to give a sincere thank to Associate Professor Bunjerd Jongsomjit, the chairman of the committee for this thesis, Associate Professor Anongnat Somwangthanaroj as the examiner, and Assistant Professor Okorn Mekasuwandamrong as the external examiner for their comments and recommendations.

Lastly, financial supports from the Thailand Research Fund (TRF) and the Grant for International Research Integration: Chula Research Scholar, Ratchadaphiseksomphot Endowment Fund are gratefully acknowledged.

CONTENTS

Page

Page

Page

LIST OF TABLES

page

LIST OF FIGURES

page

CHAPTER I

INTRODUCTION

1.1 Introduction

The liquid phase chemoselective hydrogenation of nitroanilines is essentially utilized in industrial production of valuable intermediates for agrochemicals, pharmaceuticals, pigments, polymers, dyes, and other fine chemicals [1-3]. The liquid phase selective hydrogenation of nitrostyrene has been carried out using Pt, Au, and Pd catalysts supported on TiO_2 and high conversion (nearly 100%) with supreme selectivity to vinylaniline (73-98%) has been achieved [1, 4-6], In an earlier study by Serna P. et al.[7], TiO_2 supported bimetallic gold - platinum was synthesized by a deposition - precipitation technique and increasing of Pt content in Au@Pt/TiO_2 can enhance TOF but the chemoselectivty to reduce the nitro group decreased for Pt content over 100 ppm.

It is known that the catalytic behavior of metal that strongly interact with a support is essentially different from that of the same metal supported on inert carriers such as SiO_2, Al_2O_3 or C. Due to the strong metal support interaction (SMSI) effect, TiO_2 can enhance the selectivity and reaction rate when compared to the other supports in the liquid phase hydrogenation of 3-nitrostyene [2]. Makosch M. et al.[5] studied a new simple surface modification procedure for supported Pt particles on TiO_2 by employing organic thiols in the liquid phase selectively hydrogenation of 4-nitrostyrene to 4-aminostyrene. The use of 1, 6-dithiolhexane gave the highest rate at 0.01 mmolgcat^{-1}s^{-1} with 98% selectivity to 4-vinylaniline. The Pt-based intermetallic catalysts have been synthesized using a wide range of synthesis techniques such as incipient wetness impregnation, slurry synthesis method, electroless deposition, and dendrimer support synthesis. The selective hydrogenation reactions over Pt-based bimetallic catalysts have also been carried out by using various catalyst systems such as Pt-Ni/γ-Al_2O_3 , Pt-Co/γ-Al_2O_3 , , Pt-Pd/γ-Al_2O_3 , Pt-Au/SiO_2 , Pt-Cu/SiO_2 , Pt-Fe/SiO_2 ,

Pt-Zn/TiO_2 , Pt-Ga/CNF , and Pt-Ru/CNT [8].

In the present work, we synthesized a group of Pt based bimetallic catalysts with other transition metals supported on titania by incipient wetness impregnation method and varied the content of second metals in the liquid phase selective hydrogenation of 3-nitrostyrene to 3-vinylaniline.

1.2 Research Objectives

The objectives of research have allocated into 2 parts as follows :

Part I : To investigate the characteristics and catalytic properties of the Pt based bimetallic catalysts prepared by co-impregnation method in the liquid phase selective hydrogenation of 3-nitrostyrene to 3-vinylaniline

Part II : To study the effect of selected second metal content on the bimetallic catalysts in the liquid-phase selective hydrogenation of 3-nitrostyrene.

1.3 Research Scope

This research scope is to synthesize Pt/TiO_2 and Pt based bimetallic /TiO_2 : The scope details are listed below.

1) Synthesis of 0.5wt%Pt/TiO_2 by employing the incipient wetness impregnation method using aqueous solution of H_2PtCl_6 * $6H_2O$ precursor.
2) Synthesis of 0.5wt% Pt with another transition metal to made bimetallic catalysts with the same loading wt% of metal deposit by co-incipient wetness impregnation method.
3) Synthesis of 0.5wt% Pt with various contents of the selected other transition metal from 0.2 to 0.7 wt% to made bimetallic catalysts.
4) Calcination in air at 450°C for 2 h and then reduction in H_2 flow at reduction temperature around 200°C.

5) Reaction study of Pt/TiO_2 catalysts and Pt based bimetallic catalysts in the liquid phase chemoselective hydrogenation of 3-nitrostyrene to 3-vinylaniline in a stirred stainless steel autoclave reactor at 2 MPa of H_2 pressure and 40°C for 0.5 to 3 hours.

6) Characterization of TiO_2 , Pt/TiO_2 catalyst , Pt based intermetallic catalysts by using diversified techniques such as :

- H_2 temperature program reduction (H_2-TPR)
- CO Pulse Chemisorption
- X-ray diffraction (XRD)
- Surface area and Porosity Analysis (BET)
- CO impulse infrared spectroscopy (CO-IR)
- X-ray photoelectron spectroscopy (XPS)
- Scanning Electron Microscope (SEM)

1.4 Research methodology

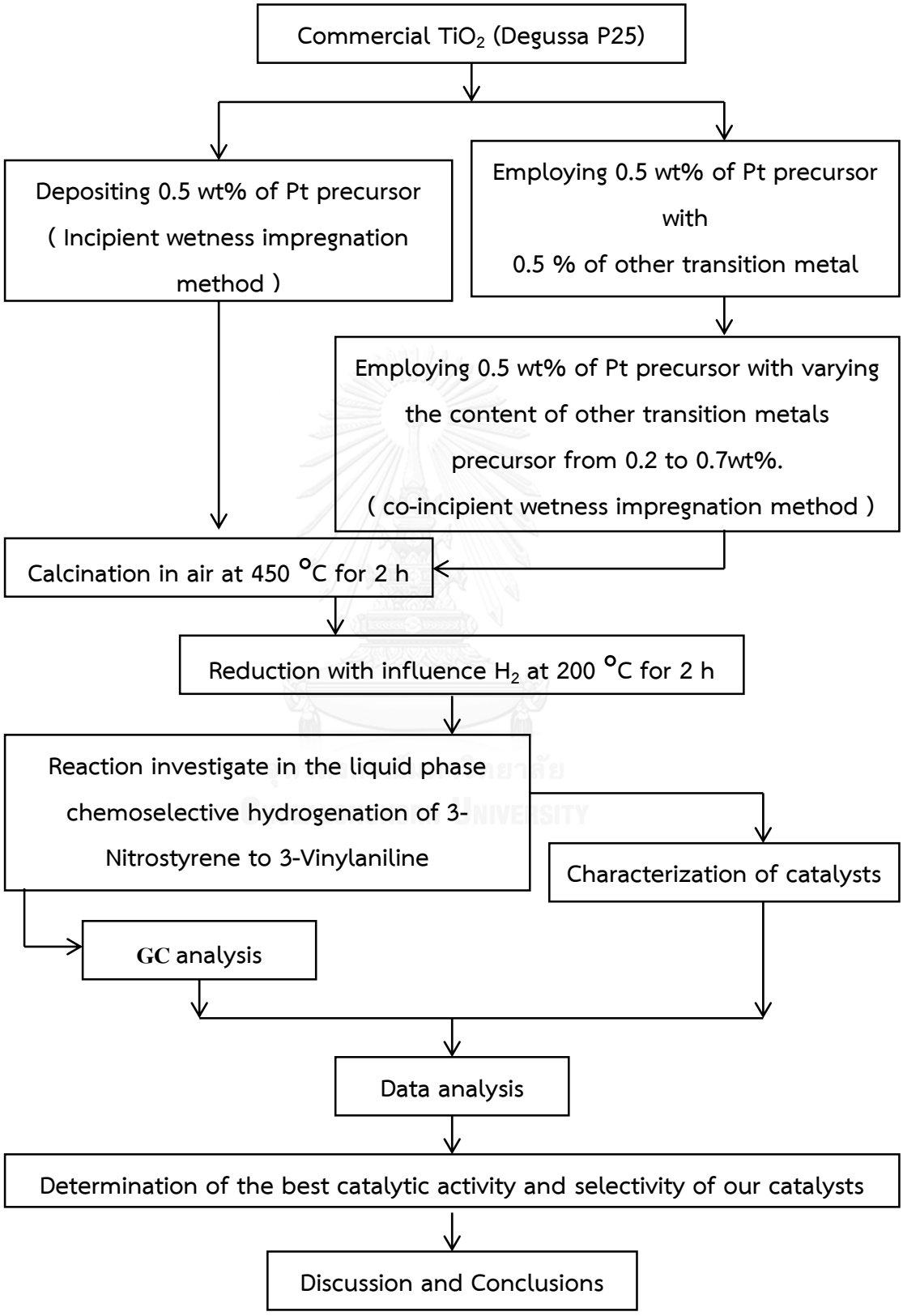

CHAPTER 2

THEORY AND LITERATURE REVIEWS

The crucial information for carrying out the liquid phase selective hydrogenation of 3-nitrostyrene such as data of support material, incipient wetness impregnation method, catalyst metal, and literature reviews are provided in this section.

2.1 Titanium dioxide (TiO_2)

Titanium dioxide is the most eminent oxide materials for proceeding industrial applications combined to corrosion protective coating, white pigment in planting, waste water treatment, and photo-catalysts for pollutant removal from the air. Further utilization consist of food additive, cosmetic, sensors, part of photovoltaic devices, and especially catalyst support (increase catalyst surface area, TiO_2 induce in changes of catalytic activity and selectivity, and change in catalytic properties has been attributed to the strong-metal support interaction effect (SMSI)). Three polymorphs of titania occur in nature: rutile (tetragonal), anatase (tetragonal) and brookite (orthorhombic) [9-11] Rutile is the only stable phase whereas anatase and brookite are metastable at all temperatures, transforming to rutile when they are heated. Their properties of rutile, anatase and brookite TiO_2 are shown in Table 1 [12]. And crystalline structures are demonstrated in **Figure 1** [9].

Table 1 The electronic properties of three main polymorphs of TiO_2 (rutile, anatase, and bookite)

Polymorph	Rutile	Anatase	Brookite
Crystal structure	tetragonal ,$P4_2/mnm$	tetragonal , $I4_1/amd$	orthorhombic , Pcab
Density (kg/m^3)	4.25	3.89	4.12
Reflection index (λ=600nm)	// to c axis 2.89	// to c axis 2.48	// to c axis 2.69
Dielectric constant	// to c axis 173	// to c axis 48	78
Band gap (eV)	// to c axis indirect 3.05	// to c axis indirect 3.46	3.14
Electron mobility (10^{-4} m^2/Vs)	crystal : 0.1-10 thin film : 0.1	crystal : 15-550 thin film : 0.1-4	

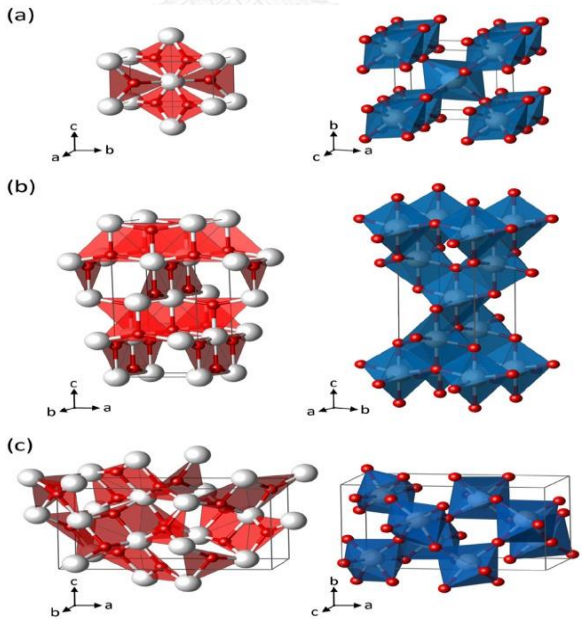

Figure 1 Planar Ti_3O building-block representation (left) and TiO_6 polyhedra (right) for the TiO_2 phases rutile (a), anatase (b) and brookite (c) (Ti (white); O (red))

The experimental lattice parameters $a = b = 4.5937$ A°, $c = 2.9581$ A° for rutile $a=b=3.7842$A° $c=9.5146$A° for anatase and $a=9.16$A°, $b=5.43$A°, $c=5.13$A° for brookite have been revealed in previously. Nevertheless, the electro chemical and the physical properties of titanium dioxide such as the crystal structure , morphology ,and particle size are rely on the preparation method that covering of hydrothermal, sol-gel, chemical vapor and physical deposition, solvothermal, electrochemical approaches, solution combustion, and microemulsion techniques.

2.2 Platinum catalyst

Platinum metal (Pt) has been utilized as a traditional active metal in liquid phase selective hydrogenation of nitroaromatic compounds by promoting or using as a bimetallic catalyst with other metal such as, Au and Co. Preparation of Pt catalysts have been reported. They have been deposited on TiO_2, SiO_2, γ-Al_2O_3, and actviated carbon by different methods, for examples: impregnation, deposition-precipitation, colloid deposition, and ionic liquid method [1, 2, 5-7, 13]

2.2.1 Incipient wetness impregnation method

Incipient wetness impregnation is the most commonly utilized method because of its easy way to do in sample preparation. The cluster of precursor required is estimated based on the desired metal loading for each catalyst. To synthesize the catalyst, a metal precursor is dissolved in a solvent (deionized water is the most generally used solvent for wet impregnation). When the precursor is completely dissolved, the solution is drop-wised gently to the support. Capillary action carries the aqueous solution up into the pores of the support where the metal precursor is deposited. Then the catalyst was dried at desired temperature to remove solvent for several hours. After that, the catalyst was calcined at high temperature to vaporize the nonmetallic components of the precursor salt, leaving the metal in an oxidized state on the support surface [8].

2.3 Bimetallic catalysts

Heterogeneous bimetallic alloy catalysts, usually present electronic and chemical properties that are different from those of their parent metals, propose the chance to obtain new catalysts with improved selectivity, activity, and stability. Recently, bimetallic catalysts are broadly utilized in many catalytic and electro-catalytic applications. It is well-known that bimetallic surfaces often exhibit novel properties which are not present on either of the parent metal surfaces [14-16].

The modification of the electronic and chemical properties of a metal in a bimetallic surface arise from two significant determinants. First, the formation of heteroatom bonds changes the electronic environment of the metal surface, presenting rise to modifications of their electronic structure during the ligand effect. Second, the geometry of the bimetallic structure is typically different from the parent metals [8].

2.4 Selective hydrogenation reaction of 3-nitrostyrene

Selective hydrogenation of a nitro group (NO_2) and vinyl group (C=C) is an addition of H_2 atoms to a C=C either or N=O double bond for generate nitro group product. The ordinary source of two hydrogen atoms is molecular hydrogen (H_2). Although, a careful hydrogenation proceeds is very rapidly hydrogenated to a nitro group product. Then the overall hydrogenation reaction is exothermic, the high activation energy also prevents it from taking place under normal conditions. **Figure 2.** exhibited the reaction path way of 3-nitrostyrene that can be transformed into 3 main products as a vinilaniline or aminostyrene (VA or AS), ethylnitrobenzene (ENB), and final product ethylaniline (EA) [17].

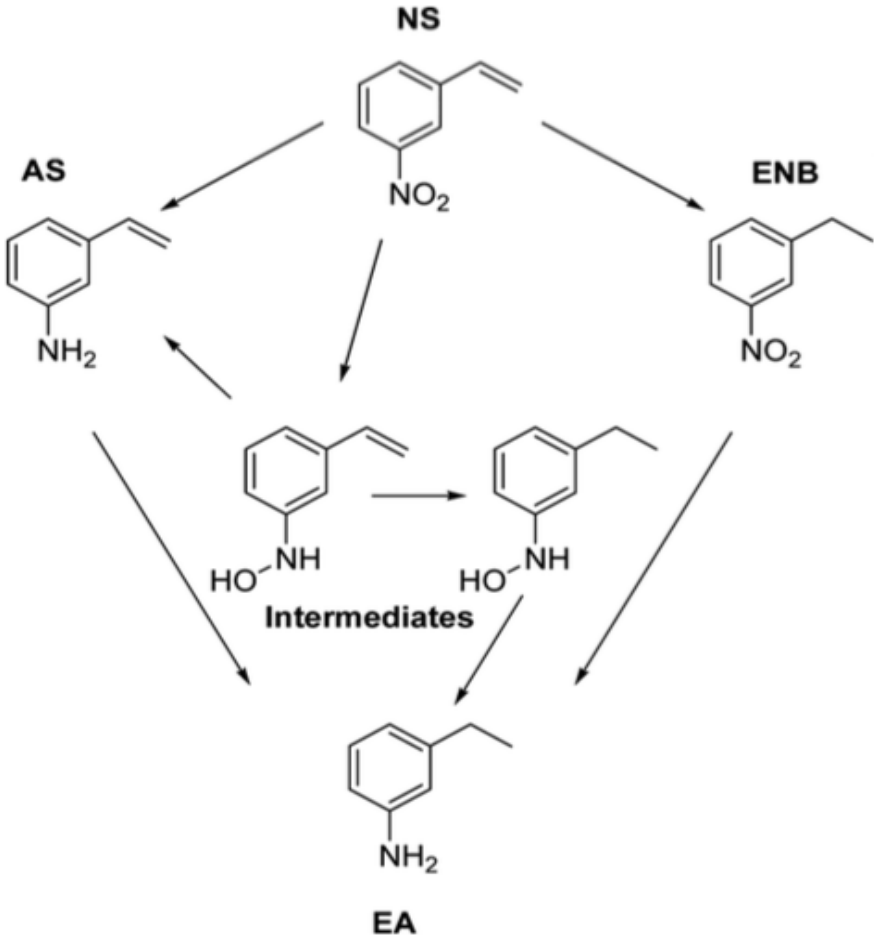

Figure 2. The hydrogenation pathways of 3-nitrostyrene focused on product of reaction mixture

2.5 Literature reviews

2.5.1 Selective hydrogenation of nitrostyrene using different catalysts

Boronat M. et al. (2007) showed that Au/TiO_2 achieved very high chemoselectivity for liquid phase hydrogenation of the nitro group in 3-nitrostyrene at conversion nearly 100% when compare with Pt/TiO_2 and Pd/TiO_2 catalysts. On the other hand, Pt/TiO_2 had particularly active for catalyze vinyl group (C=C) hydrogenation. TiO2 was active support for Au catalyst that can achieved conversion and selectivity of 3-Nitrostyrene higher (98.5% conversion and 96 % selectivity of 3-vinylaniline in 6 h) than other support. Metal oxides such as TiO_2 and Fe_2O_3 improved role for favored reducing the nitro group, that can't be accomplished by utilizing "innert " support (SiO_2 and C).

Serna P. et al. (2009) studied bimetallic gold – platinum that was synthesized by a deposition – precipitation technique and kinetic models. The catalytic results during the liquid phase hydrogenation of 3-Nitrostyrene using different Au and Pt catalysts appear that 0.2% Pt/TiO_2 under reaction temperature 85 ℃ and H_2 pressure 0.8 M Pa showed supreme catalytic activity (95.1 % conversion and 69.7% selectivity of vinylaniline) in 15 min but 1.5% Au/TiO_2 at the same conditions demonstrated slightly increase of nitrostyrene conversion and accomplished 96.2% selectivity of vinylaniline in 9 h. while intermetallic 1.5% Au@ 0.01% Pt/TiO_2 gave brilliant catalytic activity (94.5% conversion and 93.4 % selectivity of vinylaniline) in 31.2 min. In addition , increasing of Pt content in Au@ Pt/TiO_2 can enhance TOF but the chemoselectivty to reduce the nitro group decreased for Pt content over 100 ppm.

Fujita S. et al. (2011) presented effect of pressurized carbon dioxide ($ScCO_2$) and catalyst preparation conditions. At first, the influence of solvents on the hydrogenation of nitrostyrene with Pt/TiO_2 showed that the use of ethanol gave the highest conversion of nitrostyrene at 99% but the selectivity to vinylaniline was low (48% selectivity). In contrast, $scCO_2$ improved the selectivity of vinylaniline to 75% but conversion of nitrostyrene was not high (64% conversion). The influence of CO_2 pressure increased conversion of nitrostyrene up to 12 MPa; however, it was decreased with further increase of CO_2 pressure. To illustrate the cause of pressure dependence, the liquid phase of nitrostyrene slightly expanded with increasing of CO_2 pressure and the liquid – gas two phases turned to single phase at 13.5 MPa, unveiling H_2 was absolutely dissolved in CO_2 phase resulted in the decrease of the 3-nitrostyrene conversion. Under CO_2-dissolved expanded liquid (CXL) conditions, dissolved CO_2 can enhanced the disunion of H_2 into the liquid phase. This possibly reason for increase of nitrostyrene conversion under 12 MPa. The selectivity to vinylaniline was slightly increase with increasing of CO_2 pressure up to 10 MPa. Over this pressure, the selectivity to vinylaniline was decreased. On the other hand, the selectivity to ethylnitrobenzene increased at CO_2 pressure above 10 MPa. Effect of Pt loading on catalytic activity of Pt/TiO_2 was examined in the residence of CO_2 pressure (10 MPa), the increase of Pt loading can enhance activity of catalyst from 64% to 94% conversion of nitrostyrene. Although the selectivity to vinylaniline was declined by Pt loading from 75% to 34% selectivity of vinylaniline. The effect of reduction temperature on the performance of 0.5 wt% Pt/TiO_2 for the hydrogenation of nitrostyrene was investigated, catalyst reduce at higher temperature over 473 K exhibited higher selectivity to vinylaniline. Despite, their conversion of nitrostyrene were lower. The catalyst reduced at 723 K gave the best selectivity to vinylaniline at 94%.

Serna P. et al. (2011) reported the deposition precipitation technique of gold nanoparticle onto the surface of TiO_2 (Degussa, P-25) and the incipient wetness technique of Pt with various supports such as γ-Al_2O_3, Activated carbon and TiO_2 supports. The catalytic results for the hydrogenation of 3-nitrostyrene using Au/TiO_2 catalysts with increase average particle size exhibited the highest yields from small particle diameter of 3.8 and 5.8 nm, 60.3% and 57.7% respectively, and the activity continuously decrease for particle size larger than 8.5 nm. Although, the selectivity to vinylaniline are almost same advising that particle shape of Au may an important factor for nitrostyrene hydrogenation. The strong metal support interactions (SMSI) effect is reflected in changes in the electronic density of small clusters, in generation of special active sites at the metal-support boundaries. The selectivity toward 3-vinylaniline obtained from 0.2% Pt/TiO_2 (activated at 450°C) catalyst was slightly decrease with increasing of conversion of 3-nitrostyrene while other catalysts such as 0.2% Pt/TiO_2 (activated at 200°C) , 2% Pt/TiO_2 (activated at 450°C) and 2% Pt/TiO_2 (activated at 200°C) were significantly decreased. In addition, 0.2% Pt/TiO_2 (activated at 450°C) gave highest conversion of nitrostyrene and selectivity to 3-vinylaniline (nearly 100%).

Makosch M. et al. (2012) studied a new simple surface modification procedure for supported Pt particles on TiO_2 employing organic thiols to liquid phase selectively hydrogenation of 4-nitrostyrene to 4-aminostyrene. All the Pt/TiO_2 catalyst were synthesized via incipient wetness impregnation method. The reaction carried out for all different organic thiols modification during the liquid phase hydrogenation of 4-nitrosytrene, the rate at 40 % conversion of unmodified Pt/TiO_2 catalyst was the highest noticed of all the catalysts, suggesting that the thiols block part of the surface of the Pt nanoparticles active sites. The alteration of structure affected the selectivity: that thiol containing polar groups (thioglycerol, 1,6-hexanedithiol and α- lipoic acid) yielded 100 % selectivity towards 4-aminostyrene whereas an unpolar modifier (1-dodecanethiol) yielded only 88 % selectivity. This tendency was observed at conversion level nearly 100 %. The catalyst modified with α-lipoic acid showed 100%

selectivity to 4-aminostyrene followed by 1, 6-hexanedithiol (98 %) and thioglycerol (97 %). The rate comparing with different modifiers, it was found 1, 6-dithiolhexane gave the highest rate at 0.01 mmolgcat^{-1}s^{-1} (98% selectivity to 4-vinylaniline). The stability test of catalyst was carried out in 3 cycles, the results showed the conversion of 4-nitrostyrene and selectivity to 4-vinylaniline were slightly decreased.

Furukawa S. et al. (2014) studied Pd- and Rh-based Intermetallic compounds supported on SiO_2 that were synthesized via pore-filling impregnation technique and investigated on CTH Reaction of nitrobenzene and nitrostyrene. The formation of the intermetallic compounds made a structure of two metal elements into coadjacent at the atomic level on the surface of the nanoparticles. Increasing in the electronegativity of the second metal element gave polar sites and enhanced the activation of methanol as a hydrogen donor, that accelerated the hydrogenation of the nitro group of nitrostyrene and accordingly enhanced the yield of aminostyrene. Rh-based intermetallic catalysts gave 4-aminostyrene with highly selectivities but very low catalytic activity were obtained except $RhPb_2$ intermetallic catalyst exhibited high conversion of 4-Nitrostyrene at 94%. $Pd_{13}Pb_9$ showed the highest chemoselectivity of nitrostyrene to aminostyrene (96%) in 6 h.

Fujita S. et al. (2014) reported an activated carbon (AC) catalysts that were treated by hydrogen peroxide and ammonia to dope oxygen and nitrogen on their surface. The catalytic test by hydrazine using different carbon catalysts showed conversion was significantly enhanced to 97% on the AC treated with hydrogen peroxide. Moreover, the treatment caused a significant change in the product selectivity. Additional treatment with ammonia at 600 °C gave slightly decrease of 3-nitrostyrene conversion (93%) while the selectivity to 3-vinylaniline was highly increased from 29 to 54%.

Pisduangdaw S. et al. (2014) synthesized Pt/TiO_2 catalysts for the liquid-phase selective hydrogenation of 3-nitrostyrene via flame spray pyrolysis (FSP) method. The crystallite size of F-Pt/Ti was slightly increased from 20 to 22 nm although % anatase decreased from 91 to 73% after reduction at 200–600 °C. After reduction at 700 °C, the anatase phase was completely transformed to the rutile-phase and the crystallite size increased mightily from 22 to 48 nm. For several reduction temperatures applied, the F-Pt/Ti catalysts exhibited much higher catalytic activity than the I-Pt/Ti catalysts, that was able to ascribed to the higher Pt dispersion. The catalytic efficiency of F-Pt/Ti catalyst in terms of conversion and selectivity to 3-vinylaniline were enhanced from 61 to 66% and 39 to 73% respectively, with increasing of reduction temperature to 500 and 600 °C. At higher reduction temperature except 700 °C, the decrease in Pt terrace atoms as well as the formation of $Pt–TiO_X$ sites favored VA formation.

Pisduangdaw S. et al. (2014) showed $Pt–Co/TiO_2$ bimetallic catalysts which synthesized by flame spray pyrolysis for liquid phase hydrogenation of 3-nitrostyrene with constant Pt content at 0.5 wt.% and Co concentration varying between 0.1 and 0.5 wt.%. The catalytic results when reduced at 200 °C, exhibited the increasing of ENB selectivity to 62.8% (maximum) at 0.2 wt% Co (ENB/ VA ratio = 2.1). Thus, the addition of cobalt resulted in an increased ratio of CO adsorbed on Pt terrace to corner atoms.

2.5.2 Pt-based bimetallic catalyst

Yu W. et al. (2012), The Pt-based bimetallic catalysts have been synthesized using a wide range of synthesis techniques such as Incipient wetness impregnation, slurry synthesis method, organometallic cluster precursors, reductive deposition precipitation, electroless deposition, colloidal synthesis, core-shell synthesis, reverse micelle synthesis, and dendrimer support synthesis. The utilization of Pt-based intermetallic catalysts have been divided by the catalytic reactions into several categories including hydrogenation, dehydrogenation, reforming, and oxidation reactions. Catalytic hydrogenations are among the most commonly practiced catalytic processes, ranging from common steps in organic synthesis to batch processes in pharmaceutical production, for stabilization of edible oils and petroleum upgrading processes. Because hydrogenation reactions are typically exothermic, it is advantageous to carry out these reactions at low temperatures. The selective hydrogenation reactions over Pt-based intermetallic catalysts has been carried out by using various catalyst such as Pt-Ni/γ-Al_2O_3, Pt-Co/γ-Al_2O_3, Pt-Mo/γ-Al_2O_3, Pt-Pd/γ-Al_2O_3, Pt-Ru/γ-Al_2O_3, Pt-Au/SiO_2, Pt-Cu/SiO_2, Pt-Sn/SiO_2, Pt-Fe/SiO_2, Pt-Rh/AC, Pt-Zn/TiO_2, Pt-Ge/TiO_2, Pt-Re/TiO_2, Pt-Ga/CNF, Pt-Mn/CNT, and Pt-Ru/CNT. In C=C hydrogenation, for example, cyclohexene hydrogenation were performed on Pt-Co and Pt-Ni/γ-Al_2O_3 catalysts. Cyclohexene is used as a probe molecule to study hydrogenation because cyclic hydrocarbons are important reaction intermediates in many refinery and petrochemical processes, in addition to serving as building blocks for many chemicals produced in the chemical industry. Moreover, cyclohexene has several competitive reaction pathways, including decomposition, dehydrogenation, disproportionation (self-hydrogenation), and hydrogenation. Comparative studies of these reaction pathways provide an opportunity to determine how the formation of bimetallic bonds affects the hydrogenation activity and selectivity. In addition, N=O hydrogenation of nitriles is an important industrial process to manufacture the nylon monomer, hexamethylenediamine, from adiponitrile. The studies on Pt-Ru/γ-Al_2O_3 for the hydrogenation of N=O in 2, 5-dichloronitrobenzene showed high activity and selectivity.

CHAPTER 3

EXPERIMENTAL

This section describes the research methodology for preparation of the supports, the monometallic Pt, and Pt based intermetallic catalysts with other transition metals. The catalysts were characterized with techniques consisting of H_2 temperature program reduction (H_2-TPR), CO chemisorption, X-ray diffraction (XRD), surface area and porosity analysis (BET), scanning electron microscope (SEM), CO-impulse infrared spectroscopy (CO-IR), X-ray photoelectron spectroscopy (XPS), and gas chromatography was used to analyze the products of reaction.

3.1 Chemicals

The chemical reagents used in catalyst preparation is shown below

Table 2 The reagents used in catalyst preparation

Reagent	Chemical name	Purity (%)	Suppliers
$H_2PtCl_6 \cdot 6H_2O$	Chloroplatinic acid hexahydrate	37.50	SIGMA-ALDRICH
$Fe(NO_3)_3 \cdot 9H_2O$	Iron(III) nitrate nonahydrate	99.95	SIGMA-ALDRICH
$Co(NO_3)_2 \cdot 6H_2O$	Cobalt(II) nitrate hexahydrate	98.00	SIGMA-ALDRICH
$Zn(NO_3)_2 \cdot 6H_2O$	Zinc nitrate hexahydrate	99.00	SIGMA-ALDRICH
$Ga(NO_3)_3 \cdot xH_2O$	Gallium(III) nitrate hydrate	99.00	ALDRICH
$Cu(NO_3)_2 \cdot xH_2O$	Copper(II) nitrate hydrate	99.00	ALDRICH
$Ni(NO_3)_2 \cdot 6H_2O$	Nickel(II) nitrate hexahydrate	99.99	ALDRICH
$Cr(NO_3)_3 \cdot 9H_2O$	Chromium(III) nitrate nonahydrate	99.99	ALDRICH

3.2 Synthesis of Pt/TiO_2 and Pt based bimetallic/TiO_2 catalysts

The TiO_2 (Degussa P25) supported Pt catalysts were synthesized by incipient wetness impregnation method. The Pt precursor (H_2PtCl_6 . $6H_2O$) was dissolved with deionized water even to 0.5 wt% loading , then drop-wised to the TiO_2 support and grinded until homogeneous solid. Step further, the catalysts were dried at 110 °C overnight. The dried catalysts were annealed in air at 450°C for 2 h. The series of bimetallic catalyst have been synthesized by co-incipient wetness impregnation method. The catalysts were reduced under influence of H_2 for 2 h at 200 °C before use in the catalytic tests.

3.3 Catalytic reaction in the liquid phase selective hydrogenation of 3-nitrostyrene

The magnetically stirred 20 ml of Teflon lined stainless steel autoclave reactor was employed with 20 mg of reduced catalyst, 10 ml of ethanol, and 0.4 ml of 3-Nitrostyrene. The reaction performed isothermally at 50°C in water bath and 2 MPa of H_2. Afterwards H_2 was purged to vent air from the reaction system for 3-4 times. The reaction mixture was stirred continuously with magnetic stirrer. After that, the reactor was carefully depressurized and cooled to ambient temperature. Then the product was centrifuged for 5 min before analyzed by a gas chromatograph.

3.4 Catalyst Characterizations

3.4.1 H_2 temperature program reduction

The H_2-TPR measurements were carried out in a U-tube reactor. Prior to these measurements, all the catalyst samples were pretreated with a N_2 flow (25 mL/min, 1 h, 200°C). The TPR profiles were obtained by passing carrier gas (10% H_2 in nitrogen) through the catalyst samples (25 mL/min, ramping from 30 to 800 °C at 10 °C/min) using a Micromeritics AutochemiSorb 2750 system attached with ChemiSoft TPx software.

3.4.2 CO Pulse Chemisorption

The Pt active sites and the relative percentages dispersion of Pt supported catalysts were determined by CO-pulse chemisorption technique using Micromeritics ChemiSorb 2750 (pulse chemisorption system). Approximately 0.05 g of catalyst was filled in a u-tube, incorporated in a temperature-controlled oven and connects to a thermal conductivity detector (TCD). Then, helium (He) was pursed into the reactor with a flow rate 30 ml/min in order to remove remaining air. Prior to chemisorption, the catalyst was reduced in H_2 flow rate 30 ml/min) at 200 °C for 1 h. After that cooled down to room temperature under Helium flow, then CO is plus into the catalyst bed at 30 °C. The non-adsorbed CO was measured using thermal conductivity detector. Pulsing was continued until no further CO adsorption is observed. The amount of Pt metal active sites and the relative percentage dispersions of Pt were calculated from CO adsorbed based on CO: Pt ratio of 1:1.

3.4.3 X-ray diffraction (XRD)

The X-ray diffraction was used determined XRD patterns of all the supports and all the catalysts by using the SIEMENS D5000 X-ray diffractometer connected with a computer with Diffract ZT version 3.3 programs for fully control of the XRD analyzer. The experiments were carried out by using Cu Kα radiation with Ni filter in the 2θ range of 20° to 80° and resolution 0.04°. This technique is use for specify TiO_2 anatase and crystalline size of supports and catalysts.

3.4.4 Surface area and porosity analysis (BET)

The specific surface area (using the stand BET method), average pore volume, average pore size (using the BJH desorption analysis) and hysteresis loop (using the adsorption-desorption isotherms) of catalysts and TiO_2 support were measured by using the ASAP 2020-physisorption analyzer instrument. Prior to analysis, all the catalysts and TiO_2 support were thermally treated at 150°C for 1 h. Then, nitrogen adsorption-desorption isotherms were obtained at -196°C under liquid nitrogen.

3.4.5 X-ray photoelectron spectroscopy (XPS)

The XPS spectra, the binding energy, full width at half maximum (FWHM) and the composition of the Pt catalysts on the surface layer of the catalysts were performed by using the Kratos Amicus X-ray photoelectron spectroscopy. The experiment was operated with the X-ray source at 20 mA and 12 kV (240 W), the resolution at 0.1 eV/step and the pass energy of the analyzer was set at 75 eV under pressure approximately 1x10-6 Pa. For calibration, the binding energy was referenced to C 1s line at 285.0 eV. The binding energy of O 1s, Ti 2p, N 1s, and Pt 4f were determined.

3.4.6. FTIR spectra of adsorbed CO (CO-IR)

Fourier Transform Infrared spectra of adsorbed CO was performed in an FTIR-620 spectrometer (JASCO) with an MCT detector at a wavenumber resolution of 4 cm^{-1}. The samples were initially introduced with He flow in order to remove the remaining air. Then system was switched to pure H_2 flow and raised to 200°C for 1h. After reduction, the sample was cooled down to the room temperature in He flow for 30 min, followed by CO adsorption under Co/He flow for 15 min. After that, flushing the sample with He flow for 15 min before recording the IR spectrum of CO in 1600–2200 cm^{-1} range.

CHAPTER 4

RESULTS AND DISCUSSION

This chapter are comprised of two parts including the effect of different second metal on Pt based bimetallic catalysts and the effect of various amounts of selected second metal on Pt based bimetallic catalysts. The characteristics of catalysts were investigated by N_2-physisorption, XRD, XPS, H_2-TPR, CO-IR, and SEM analysis. The catalytic properties of Pt based bimetallic catalysts supported on TiO_2 P-25 supports were investigated in the liquid-phase selective hydrogenation of 3-nitrostyrene to 3-vinylaniline.

4.1 The effect of different second metals on Pt based bimetallic catalysts

The Pt based bimetallic catalysts supported on TiO_2 were prepared by co-incipient wetness impregnation methods with different second metals. The weight % of Pt and second metals were 0.5.

4.1.1 Catalysts characterization

4.1.1.1 X-ray diffraction

The XRD patterns of 0.5Pt/TiO_2 and Pt based bimetallic catalysts /TiO_2 were measured by X-ray diffraction technique in a range of diffraction angles (2θ) between 20° to 80°. **In the Figure 3. and Figure 4.** the 0.5Pt/TiO_2 and Pt based bimetallic catalysts /TiO_2 displayed the main characteristic peaks of anatase phase TiO_2 at 25.2° (major peak), 37.7°, 47.9°, 53.7°, 54.9°, 62.5°, 68.5°, 69.8°, and 74.7° with 3 peaks of rutile phase of TiO_2 [18-20]. The XRD results revealed the presence of amorphous phase when Fe, Co, or Ga were added to the Pt catalysts.

Besides, the XRD patterns of the others metal/metal oxide species were not detected.

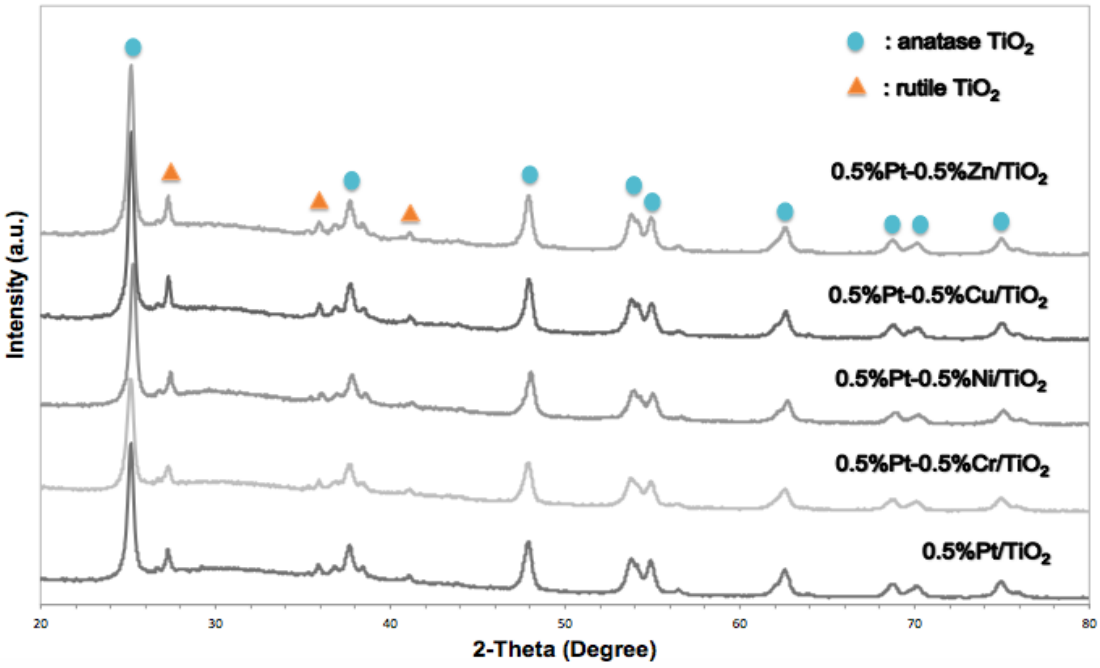

Figure 3. The XRD patterns of Pt/TiO_2 and $Pt\text{-}0.5\%X/TiO_2$ (X = Cr, Ni, Cu, and Zn) catalysts

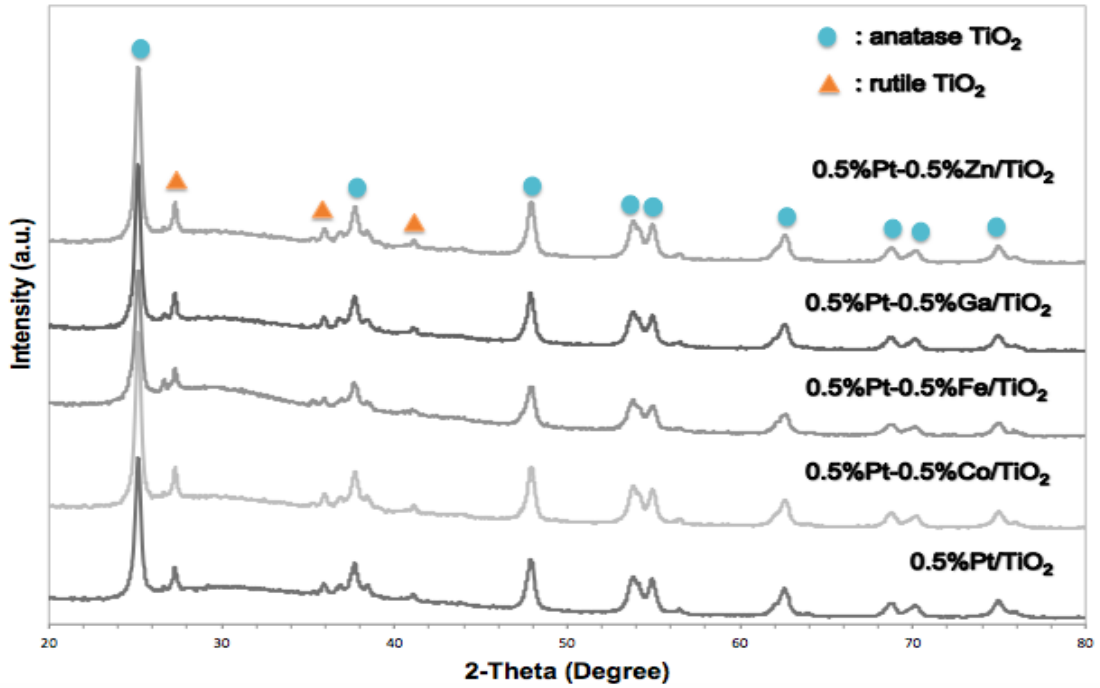

Figure 4. The XRD patterns of Pt/TiO_2 and $Pt\text{-}0.5\%X/TiO_2$ (X = Co, Fe, and Ga) catalysts

Table 3 illustrates the peak position of anatase (101) TiO_2, d-spacing and lattice parameters of the series of Pt based bimetallic over TiO_2 supports. The distance between crystals planes (d-spacing), which associated to the lattice parameters of 0.5Pt-0.5Cu/TiO_2 and 0.5Pt-0.5Ni/TiO_2 were decreased to 3.530 nm and 3.516 nm, respectively when compared to 0.5Pt/TiO_2 and could be linked to the shift of the peak position of anatase TiO_2. The lattice parameters of 0.5Pt-0.5Cu/TiO_2 and 0.5Pt-0.5Ni/TiO_2 were not changed suggesting that the metals maybe deposited on the TiO_2 surface and that there were no insertion of second metal by co-impregnation method in the TiO_2 lattice for the other Pt based bimetallic catalysts and they covered on the TiO_2 surface instead. These results unveil that addition of second metal from the 4th row of periodic table did not affect the TiO_2 lattice and the XRD diffraction peaks.

Table 3. The peak position of anatase (101) TiO_2, d-spacing and the lattice parameters of the series of Pt based bimetallic over TiO_2 supports

Catalysts	Peak position of anatase (101) (2θ, degree)	d-spacing (nm)	Lattice parameter[a] (A^0)	
			a (=b)	c
0.5Pt/TiO_2	25.16	3.535	3.792	9.772
0.5Pt-0.5Cr/TiO_2	25.18	3.533	3.794	9.689
0.5Pt-0.5Ni/TiO_2	25.30	3.516	3.791	9.409
0.5Pt-0.5Cu/TiO_2	25.20	3.530	3.791	9.682
0.5Pt-0.5Zn/TiO_2	25.16	3.535	3.791	9.798
0.5Pt-0.5Co/TiO_2	25.16	3.535	3.791	9.798
0.5Pt-0.5Fe/TiO_2	25.18	3.533	3.791	9.739
0.5Pt-0.5Ga/TiO_2	25.16	3.535	3.792	9.772

[a]calculated from Bragg's law using the diffraction peaks of anatase (101) TiO_2.

4.1.1.2 CO Chemisorption

The amounts of CO chemisorption on the 0.5Pt/TiO_2 and 0.5Pt-0.5X/TiO_2 are shown in **Table 4.** The CO chemisorption of Pt based bimetallic catalysts was measured after the catalyst were reduced with H_2 gas for 2 h. The number of surface Pt atoms on the Pt bimetallic catalysts derived from CO uptake were ranged between 7.2-14.8 x10^{18} molecules CO whereas the monometallic Pt/TiO_2 exhibited higher CO chemisorption at 13.2 x10^{18} molecules (except 0.5Pt-0.5Cu/TiO_2). It is suggested that some of Pt surface was covered by the second metal and/or alloy formation occurred, resulting in lower amount of active Pt surface. In addition, the second metal should be formed with Pt, not isolated. This is confirmed by the decrease in the amount of CO chemisorption. The calculated %Pt dispersion was decreased from the monometallic Pt/TiO_2 (85% dispersion) to 46.6-77.8% dispersion on the bimetallic catalysts. Astonishingly, 0.5Pt-0.5Cu/TiO_2 unveiled the highest CO chemisorption at 14.8 x10^{18} molecules with 96.2 % Pt dispersion but the activity of this catalyst for 3-nitrostyrene was depleted to 2% maybe because of interaction between Pt-Cu. On the other hand, 0.5Pt-0.5Co/TiO_2 unveiled the lowest CO chemisorption at 7.2 x10^{18} molecules CO.

Table 4. CO Chemisorption properties of 0.5Pt/TiO_2 and 0.5Pt-0.5X/TiO_2 catalysts

Catalysts	Volume of CO adsorption (cm^3/g)	% Dispersion	Active site (*10^{18}molecule CO/g)
0.5Pt/TiO_2	0.49	85.6	13.2
0.5Pt-0.5Cr/TiO_2	0.41	71.0	11.0
0.5Pt-0.5Ni/TiO_2	0.41	71.8	11.1
0.5Pt-0.5Cu/TiO_2	0.55	96.2	14.8
0.5Pt-0.5Zn/TiO_2	0.38	66.1	10.2
0.5Pt-0.5Co/TiO_2	0.27	46.6	7.2
0.5Pt-0.5Fe/TiO_2	0.45	77.8	12.0
0.5Pt-0.5Ga/TiO_2	0.39	67.6	10.4

4.1.1.3 H_2 temperature program reduction

The H_2-TPR measurements were performed to investigate the reduction behavior of the 0.5Pt/TiO_2 and 0.5Pt-0.5X/TiO_2 (X=Cr, Ni, Cu, Zn, Co, Fe and Ga) catalysts. **Figure 5. and Figure 6.** display the H_2-TPR profiles for 0.5Pt/TiO_2 catalysts which exhibited four district reduction peaks at 105°C, 310°C, above 450°C, and small shoulder peak around 350-400°C. The high intensity peak at 105°C could be assigned to the reduction of Pt oxide particles. Most of the Pt based bimetallic catalyst series revealed a shift of Pt reduction peak (100-230°C) to lower temperatures compared to the Pt monometallic catalyst exclude 0.5Pt-0.5Cu/TiO_2. A small shoulder peak at 350-400°C corresponded to reduction of Pt species interacted strongly with the TiO_2 support in the form of Pt-TiO_X interface sites [6]. The small peak noted at 310 °C was owing to the reduction of Ti^{4+} to Ti^{3+}. Furthermore, the broad peaks over 450°C analogous to the reduction of surface capping O_2 of TiO_2. From the peaks shift toward lower temperatures of H_2 reduction bring to the hence that additional of second metals had an effect on the reduction temperature of Pt or interacted with Pt species.

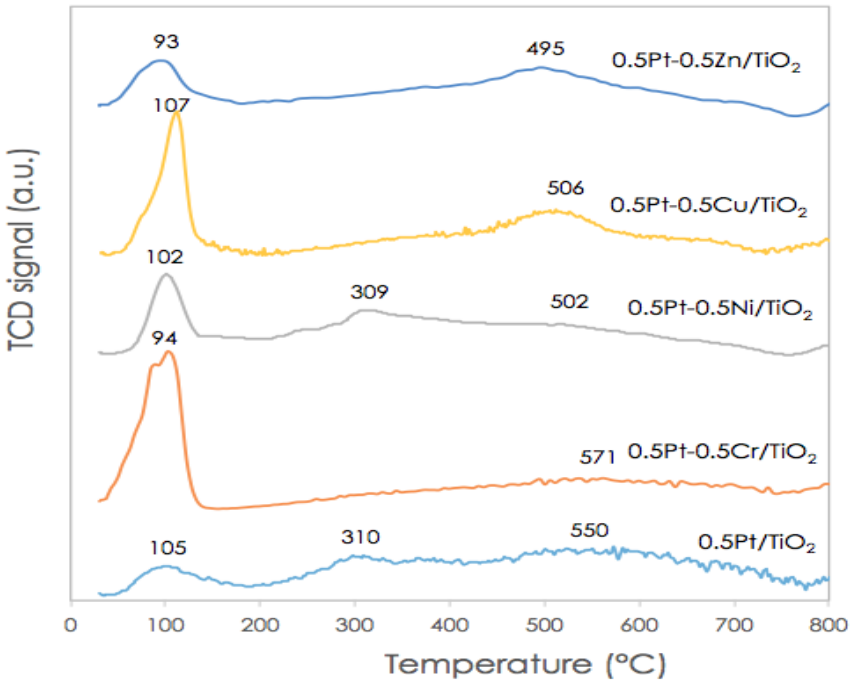

Figure 5 H_2-TPR Profile for 0.5Pt/TiO_2 and 0.5Pt-0.5X/TiO_2 (X=Cr, Ni, Cu, and Zn) catalysts

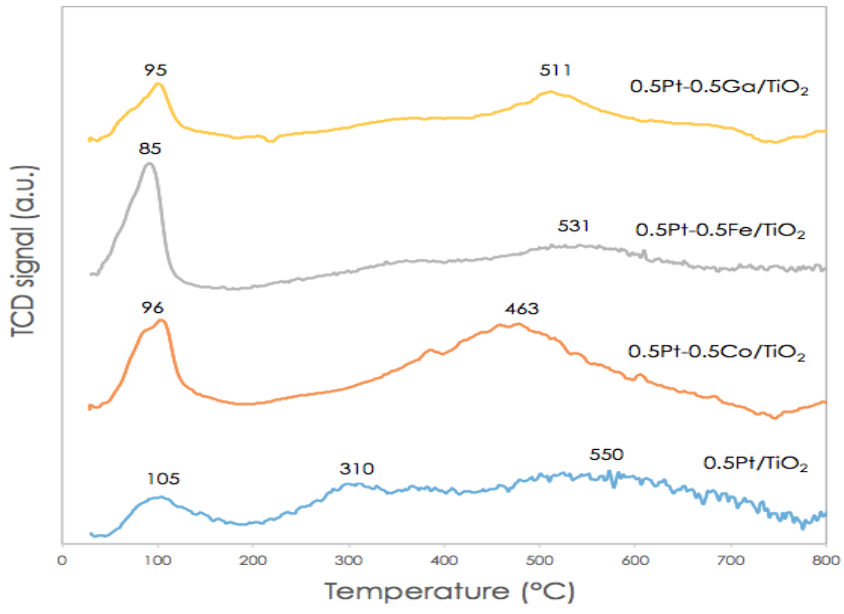

Figure 6. H_2-TPR Profile for 0.5Pt/TiO_2 and 0.5Pt-0.5X/TiO_2 (X=Co, Fe, and Ga) catalysts

4.1.1.4 Scanning electron microscopy (SEM)

The SEM images of the 0.5Pt/TiO_2 and 0.5Pt-0.5X/TiO_2 catalysts are shown in **Figure 7.** All the catalysts showed non-uniform particle size and shape. There were no significant differences in the catalyst morphology when a second metal was added by co-impregnation technique.

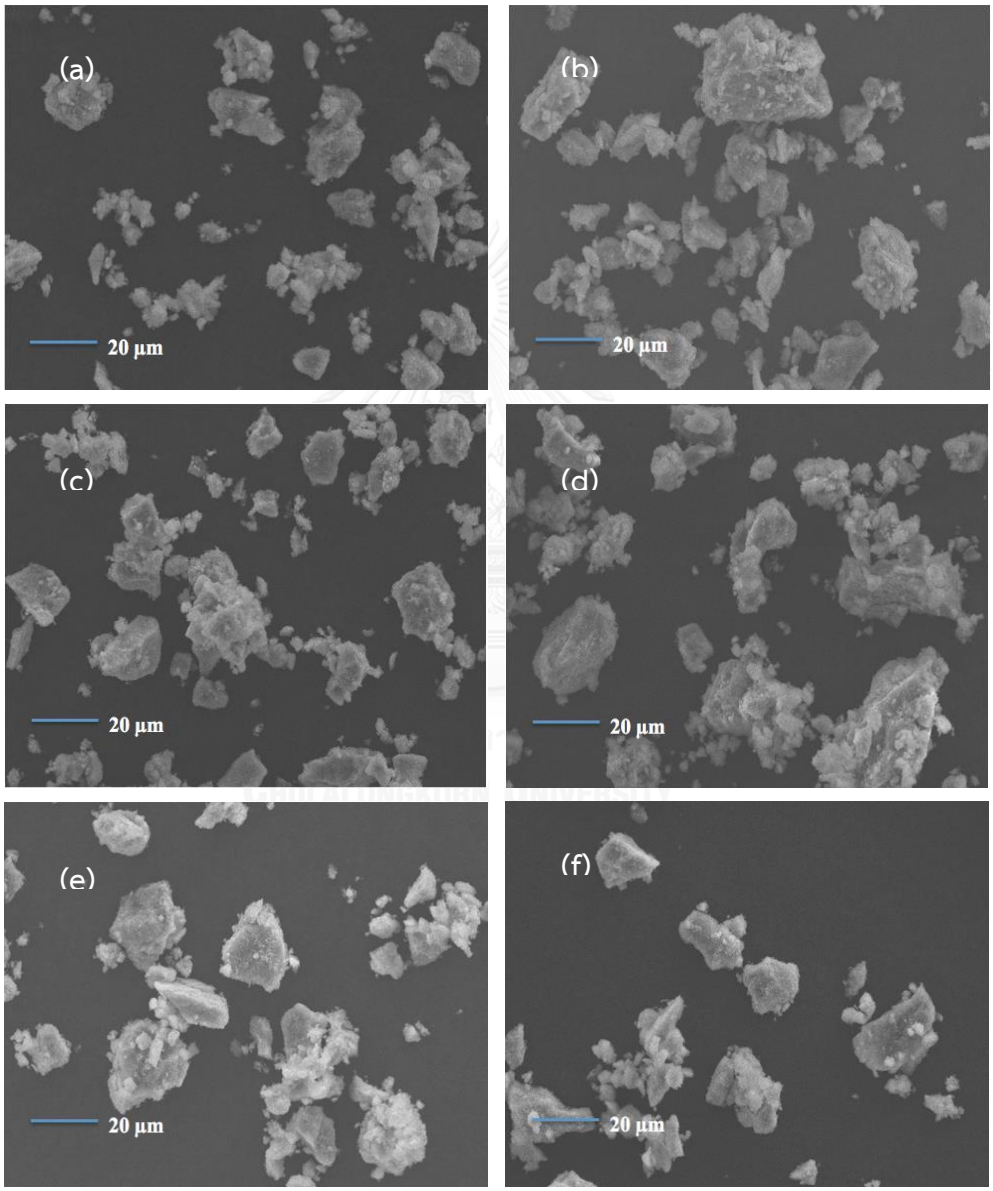

Figure 7. The SEM images of a) 0.5Pt/TiO_2 , b) 0.5Pt-0.5Co/TiO_2 , c) 0.5Pt-0.5Ga/TiO_2 , d) 0.5Pt-0.5Fe/TiO_2 , e) 0.5Pt- 0.5Zn/ TiO_2 , and f) 0.5Pt-0.5Cr/TiO_2 .

4.1.2 Catalytic activity

The obtained results for the activity of the 0.5Pt/TiO_2 and Pt based bimetallic catalysts for the liquid phase hydrogenation of 3-nitrostyrene at 50°C, 2 MPa, reaction time 1 h, using 20 ml stainless steel autoclave reactor are available in **Table 5.** The hydrogenation of 3-nitrostyrene can occur through two reaction pathways from hydrogenation of the nitro group (N=O) and the vinyl group (C=C). The conversion of 3-nitrostyrene of the Pt-based bimetallic catalysts were ranged between 1.7-96.6 %. Surprisingly, three of the bimetallic catalysts 0.5Pt-0.5Co/TiO_2, 0.5Pt-0.5Co/TiO_2, and 0.5Pt- 0.5Fe/TiO_2 with lower Pt active sites as determined by CO chemisorption results revealed higher hydrogenation activity in the 3-nitrostyrene hydrogenation than the monometallic Pt/TiO_2. These catalysts also exhibited good selectivity to 3-vinylaniline around 60-81.3 %. The addition of these second metals may modify the formation of Pt active site and/or result in an alloy formation so that their catalytic properties could be improved. The highest conversion of 3-nitrostyrene and 3-vinylaniline selectivity were observed on the 0.5Pt-0.5Fe/ TiO_2, which in accordance to the high Pt dispersion and the lowest reduction temperature in the H_2-TPR profile among the catalysts studied. Moreover, it unveiled undesired product (3-ethylnitrobenzene) with the lowest selectivity at 0.2 %. It is suggest that interaction between Pt and Fe led to promotion of hydrogenation of nitro group instead of vinyl group.

Table 5. Conversion and product selectivity for 3-nitrostyene hydrogenation over Pt/TiO_2 and Pt based bimetallic catalysts *(Reaction conditions: 2MPa of H_2 gas, 50°C, 20 mg of reduced catalyst, 10 mL of ethanol, and 1 h batch.).*

Catalyst	NS conversion (%)	Selectivity (%)			
		VA	ENB	EA	Intermediate
$0.5Pt/TiO_2$	67.7	57.6	24.9	14.5	3.0
$0.5Pt\text{-}0.5Cr/TiO_2$	29.7	52.2	29.5	8.0	10.3
$0.5Pt\text{-}0.5Ni/TiO_2$	32.6	51.5	31.6	11.0	5.9
$0.5Pt\text{-}0.5Cu/TiO_2$	1.7	57.0	28.1	7.2	7.7
$0.5Pt\text{-}0.5Zn/TiO_2$	44.3	61.4	24.0	10.3	4.3
$0.5Pt\text{-}0.5Co/TiO_2$	77.4	60.0	18.4	15.6	6.0
$0.5Pt\text{-}0.5Fe/TiO_2$	96.6	81.3	0.2	18.4	0.1
$0.5Pt\text{-}0.5Ga/TiO_2$	68.6	65.2	17.9	14.6	2.3

4.2 The effect of various amounts of second metal on Pt based bimetallic catalysts

The Pt based bimetallic catalysts supported on TiO_2 with different weight of second metals were further investigated in the 3-nitrostyrene hydrogenation. The weight % of selected second metals were ranged between 0.2-0.7%.

4.2.1 Catalysts characterization

4.2.1.1 X-ray diffraction

The XRD patterns of 0.5Pt/TiO_2 and Pt based bimetallic catalysts/TiO_2 were measured by X-ray diffraction technique in a range of diffraction angles (2θ) between 20° to 80°. In the **Figure 8. Figure 9. and Figure 10.** The 0.5Pt/TiO_2 and Pt based bimetallic catalysts with Co, Fe and Ga revealed the main characteristic peaks of anatase phase TiO_2 at 25.2° (major peak), 37.7°, 47.9°, 53.7°, 54.9°, 62.5°, 68.5°, 69.8°, and 74.7° with 3 peaks of rutile phase of TiO_2. The XRD characteristic peaks for Pt, Co, Fe, and Ga species were not detected perhaps because of low amount of their loading and/or very small metal/metal oxide crystallite size. The peak intensity of 0.5Pt-0.3Co/TiO_2 was relatively low when compared with other catalyst in Co series. For 0.5Pt-xFe/TiO_2 series, the peaks of 0.5Pt-0.2Fe/TiO_2, 0.5Pt-0.3Fe/TiO_2, and 0.5Pt-7Fe/TiO_2 became lower especially the peak of 0.5Pt-0.2Fe/TiO_2. In addition, peaks of 0.5Pt-0.2Ga/TiO_2, 0.5Pt-0.3Ga/TiO_2, and 0.5Pt-7Ga/TiO_2 also appeared in low intensity of TiO_2.

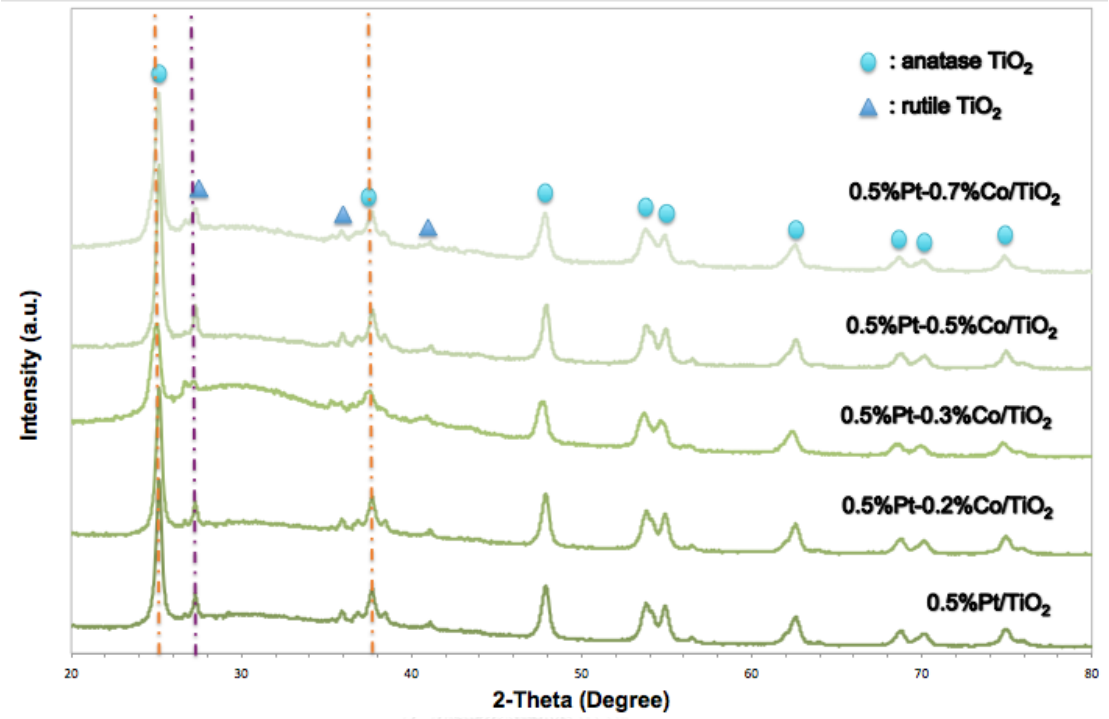

Figure 8. XRD patterns of 0.5Pt/TiO_2 and series of 0.5Pt-xCo/TiO_2 catalysts

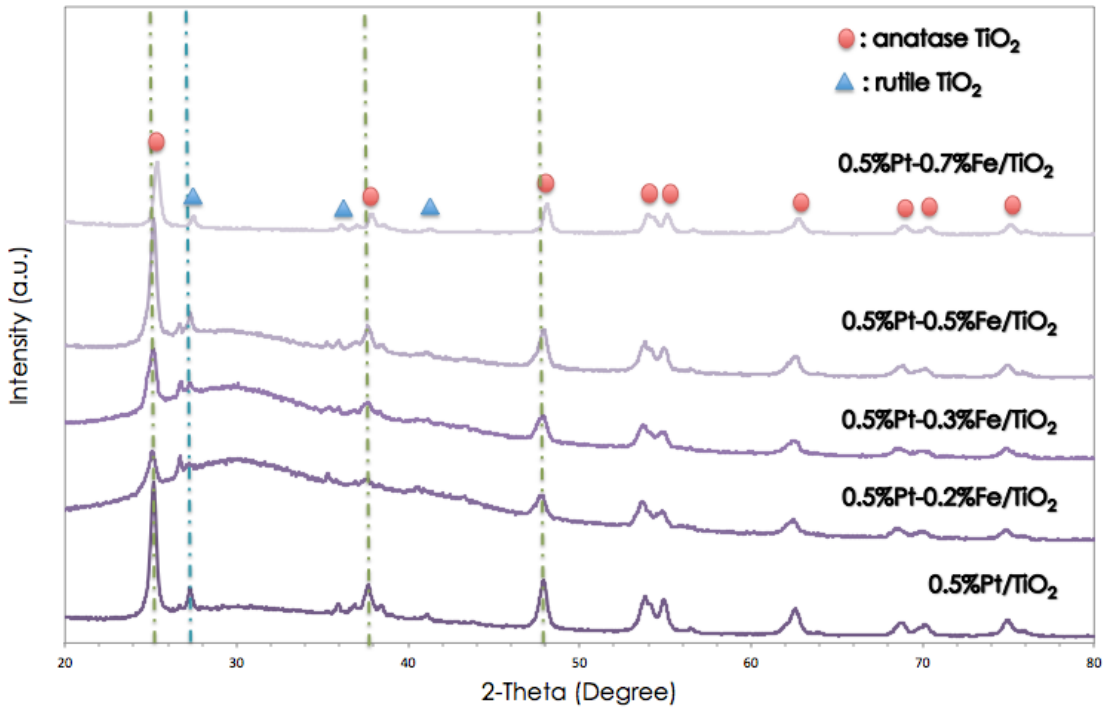

Figure 9. XRD patterns of 0.5Pt/TiO_2 and series of 0.5Pt-xFe/TiO_2 catalysts

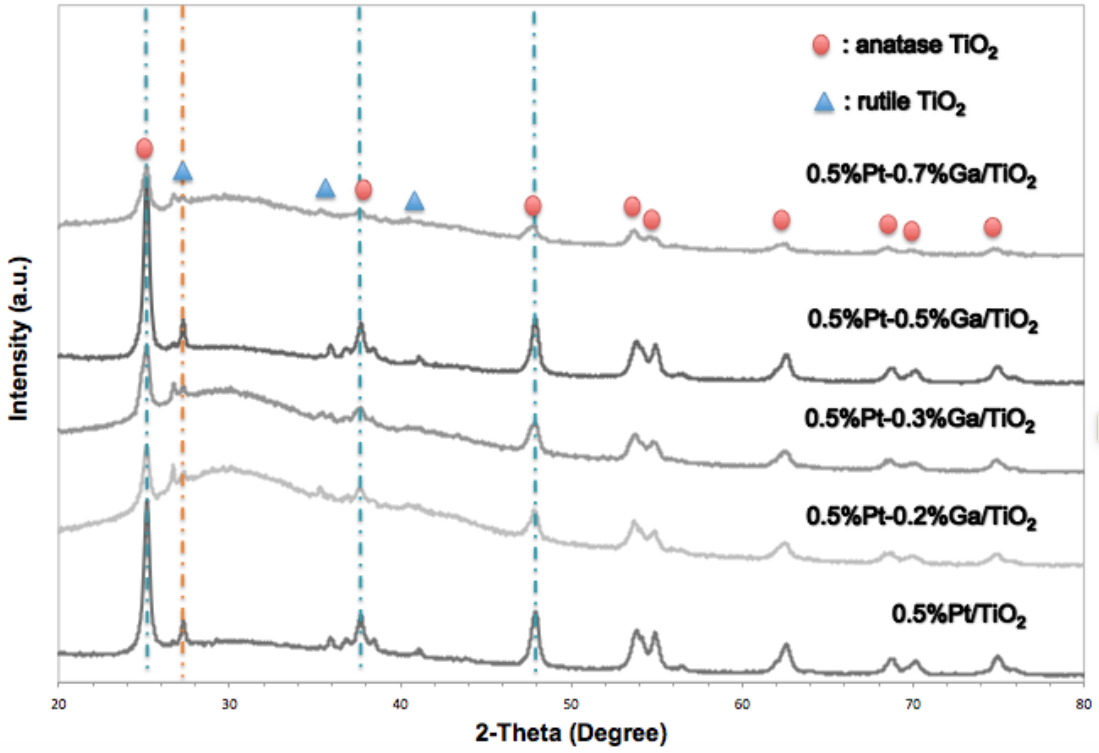

Figure 10. XRD patterns of 0.5Pt/TiO_2 and series of 0.5Pt-xGa/TiO_2 catalysts

The peak position of anatase (101) TiO_2, d-spacing and lattice parameters of the series of Pt based bimetallic over TiO_2 supports are manifested in **Table 6., Table 7.,** and **Table 8**. The peak position of anatase (101) TiO_2 of 0.5Pt-0.3Co/TiO_2 and 0.5Pt-0.7Fe/TiO_2 were shifted from 25.16° (0.5Pt/TiO_2) to 25.04° and 25.35° respectively. The distance between crystals planes (d-spacing), which associated to the lattice parameters of 0.5Pt-0.3Co/TiO_2 increased from 3.535 to 3.552 nm when compared to 0.5Pt/TiO_2. On the other hand, d-spacing of 0.5Pt-0.7Fe/TiO_2 decreased to 3.509 nm. But the lattice parameters of 0.5Pt-0.3Co/TiO_2 and 0.5Pt-0.7Fe/TiO_2 were not changed which related to coverage of metals on the TiO_2 surface. It is suggested that there were also no insertion of second metal by co-impregnation method in the TiO_2 lattice. These results revealed that addition of second metal with different amount of second metal did not have much impact on the TiO_2 lattice and the corresponding XRD diffraction peaks.

Table 6. The peak position of anatase (101) TiO_2, d-spacing and the lattice parameters of the series of 0.5Pt-xCo/TiO_2 supports

Catalysts	Peak position of anatase (101) (2θ, degree)	d-spacing (nm)	Lattice parameter[a] (A^0)	
			a (=b)	c
0.5Pt/TiO_2	25.16	3.535	3.792	9.772
0.5Pt-0.2Co/TiO_2	25.16	3.535	3.792	9.772
0.5Pt-0.3Co/TiO_2	25.04	3.552	3.806	9.895
0.5Pt-0.5Co/TiO_2	25.16	3.535	3.791	9.798
0.5Pt-0.7Co/TiO_2	25.14	3.538	3.795	9.779

[a]calculated from Bragg's law using the diffraction peaks of anatase (101) TiO_2.

Table 7. The peak position of anatase (101) TiO_2, d-spacing and the lattice parameters of the series of 0.5Pt-xFe/TiO_2 supports

Catalysts	Peak position of anatase (101) (2θ, degree)	d-spacing (nm)	Lattice parameter[a] (A^0)	
			a (=b)	c
0.5Pt-0.2Fe/TiO_2	25.14	3.538	3.809	9.558
0.5Pt-0.3Fe/TiO_2	25.14	3.538	3.798	9.729
0.5Pt-0.5Fe/TiO_2	25.18	3.533	3.791	9.739
0.5Pt-0.7Fe/TiO_2	25.35	3.509	3.778	9.472

[a]calculated from Bragg's law using the diffraction peaks of anatase (101) TiO_2.

Table 8. The peak position of anatase (101) TiO_2, d-spacing and the lattice parameters of the series of 0.5Pt-xGa/TiO_2 supports

Catalysts	Peak position of anatase (101) (2θ, degree)	d-spacing (nm)	Lattice parameter[a] (A^0)	
			a (=b)	c
0.5Pt-0.2Ga/TiO_2	25.12	3.541	3.797	9.813
0.5Pt-0.3Ga/TiO_2	25.14	3.538	3.798	9.729
0.5Pt-0.5Ga/TiO_2	25.16	3.535	3.792	9.772
0.5Pt-0.7Ga/TiO_2	25.16	3.535	3.794	9.747

[a]calculated from Bragg's law using the diffraction peaks of anatase (101) TiO_2.

4.2.1.2 CO Chemisorption

The amounts of CO chemisorption on the 0.5Pt-xCo/TiO_2, 0.5Pt-xFe/TiO_2, and 0.5Pt-xGa/TiO_2 are shown in **Table 9, Table 10, and Table 11** respectively. **T**he Pt dispersion was decreased from 71.0 % on 0.5Pt-0.2Co/TiO_2 in the order: 0.5Pt-0.2Co/TiO_2 > 0.5Pt-0.5Co/TiO_2 > 0.5Pt-0.3Co/TiO_2 > 0.5Pt-0.7Co/TiO_2. For 0.5Pt-xFe/TiO_2 series, the Pt dispersion was decreased from 77.8 % on 0.5Pt-0.5Fe/TiO_2 in the order: 0.5Pt-0.5Fe/TiO_2 > 0.5Pt-0.3Fe/TiO_2 > 0.5Pt-0.7Fe/TiO_2 > 0.5Pt-0.2Fe/TiO_2. In addition, 0.5Pt-xGa/TiO_2 series, the Pt dispersion was decreased from 66.7 % on 0.5Pt-0.5Ga/TiO_2 in the order: 0.5Pt-0.5Ga/TiO_2 > 0.5Pt-0.3Ga/TiO_2 > 0.5Pt-0.7Ga/TiO_2 > 0.5Pt-0.2Ga/TiO_2. The number of surface Pt active atoms on the Pt bimetallic catalysts derived from CO uptake were ranged between 4.7-12.0 x10^{18} molecules CO. whereas the monometallic Pt/TiO_2 exhibited higher CO chemisorption at 13.2 x10^{18} molecules, summarizing that low Pt active sites were found on 0.2, 0.3, and 0.7% loading of second metal except 0.5Pt-0.2Co/TiO_2 that demonstrated moderate Pt active sites at 11.0 x10^{18}molecules CO. It is suggested that most of Pt surface was covered by the second metal and/or alloy formation occurred, resulting in significantly low amount of active Pt surface.

Table 9. CO Chemisorption properties of 0.5Pt-xCo/TiO_2 catalysts

Catalysts	Volume of CO adsorption (cm^3/g)	% Dispersion	Active site ($*10^{18}$molecule CO/g)
0.5Pt-0.2Ga/TiO_2	0.20	34.7	5.4
0.5Pt-0.3Ga/TiO_2	0.31	53.4	8.2
0.5Pt-0.5Ga/TiO_2	0.39	67.6	10.4
0.5Pt-0.7Ga/TiO_2	0.28	48.0	7.4

Table 10. CO Chemisorption properties of 0.5Pt-xFe/ TiO_2 catalysts

Catalysts	Volume of CO adsorption (cm^3/g)	% Dispersion	Active site ($*10^{18}$molecule CO/g)
0.5Pt-0.2Co/TiO_2	0.41	71.0	11.0
0.5Pt-0.3Co/TiO_2	0.21	35.9	5.5
0.5Pt-0.5Co/TiO_2	0.27	46.6	7.2
0.5Pt-0.7Co/TiO_2	0.18	30.5	4.7

Table 11. CO Chemisorption properties of 0.5Pt-xGa/TiO_2 catalysts

Catalysts	Volume of CO adsorption (cm^3/g)	% Dispersion	Active site ($*10^{18}$molecule CO/g)
0.5Pt-0.2Fe/TiO_2	0.19	33.8	5.2
0.5Pt-0.3Fe/TiO_2	0.20	34.9	5.4
0.5Pt-0.5Fe/TiO_2	0.45	77.8	12.0
0.5Pt-0.7Fe/TiO_2	0.20	34.7	5.4

4.2.1.3 H_2 temperature program reduction

The H_2-TPR measurements were performed in order to investigate the reduction behaviors of the 0.5Pt/TiO_2, 0.5Pt-xCo/TiO_2, 0.5Pt-xFe/TiO_2, and 0.5Pt-xGa/TiO_2 (x=0.2, 0.3, 0.5, and 0.7) catalysts. **Figure 11**, displays the H_2-TPR profile of 0.5Pt-xCo/TiO_2 catalyst series. The catalyst exhibited Pt reduction peak (90-130 °C). The 0.5Pt-0.2Co/TiO_2 showed a Pt reduction temperature at 124 °C with very low peak intensity which could be related to Pt-Co alloy or Co particles covered on Pt surface. For the other 0.5Pt-xCo/TiO_2 catalysts, the reduction peak of Pt was slightly shifted to lower temperatures compared to the Pt monometallic catalyst. A broad peak around 350-400 °C was found on 0.5Pt-0.2Co/TiO_2 due to reduction of Pt species interacted strongly with the TiO_2 support in the form of Pt-TiO_X interface sites. The 0.5Pt-0.2Co/TiO_2 exhibited a stronger metal-support interaction so that it revealed higher reduction temperature peaks at 520-620°C, this peaks could be allocated to Ti^{3+} to $Ti^{<3+}$ compared to the reduction peak of Pt/TiO_2 and the other catalyst in series [21]. For the 0.5Pt-xFe/TiO_2 series, the results are shown in **Figure 12.** The reduction peak of 0.5Pt-xFe/TiO_2 shifted toward higher temperature (above 500°C) with increasing amount of second metal. It is suggested that increasing amount of Fe on the 0.5Pt/TiO_2 resulted in more difficult to reduce Pt-TiO_x species because of the strong metal-support interaction. Unusually, two distinct reduction peaks in the ranges of 550-800°C were appeared on 0.5Pt-0.7Fe/TiO_2 which could be associated to the reduction of Fe^{2+} to metallic Fe^0 as reported by H. Einaga et al [22]. A broad shoulder peak revealed between 600-750 °C was observed for the 0.5Pt-xGa/TiO_2 series which could be attributed to the reduction of Ga^{2+} to Ga^0. From **Figure 13**, the 0.5Pt-0.7Ga/TiO_2 showed very low intensity for all reduction peaks and the TiO_2 reduction peak shifted slightly towards lower temperature compared to 0.5Pt/TiO_2 to 431 °C. On the contrary, the other peaks of 0.5Pt-xGa/TiO_2 were observed at higher reduction temperature of TiO_2 which corresponding to stronger metal-support interaction.

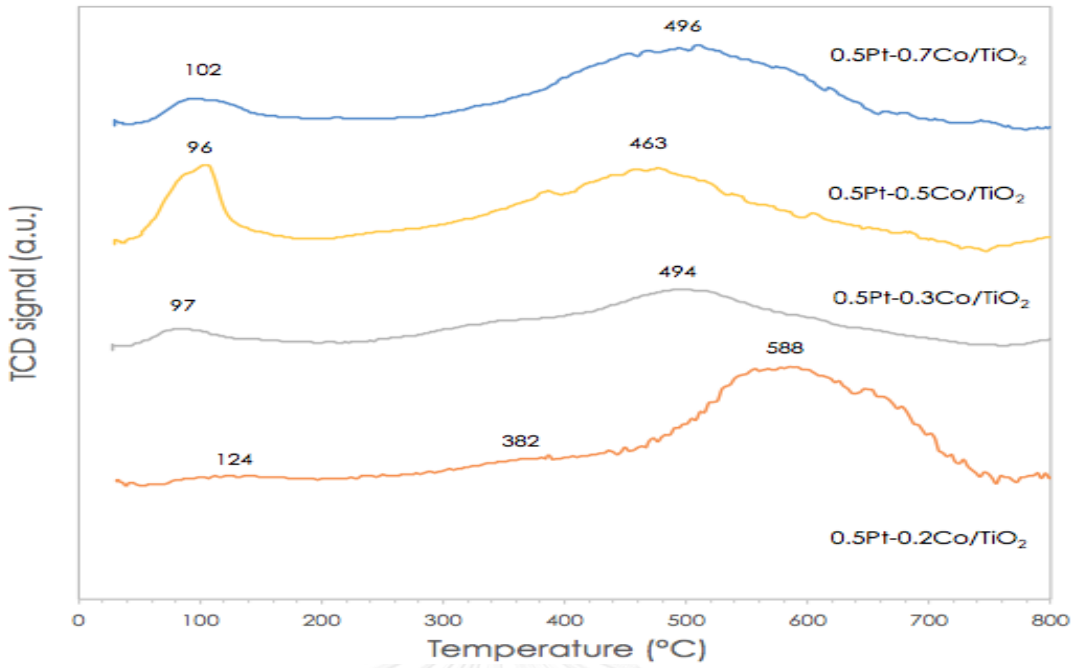

Figure 11. H_2 temperature-programmed reduction profiles of 0.5Pt-xCo/TiO_2 catalyst series.

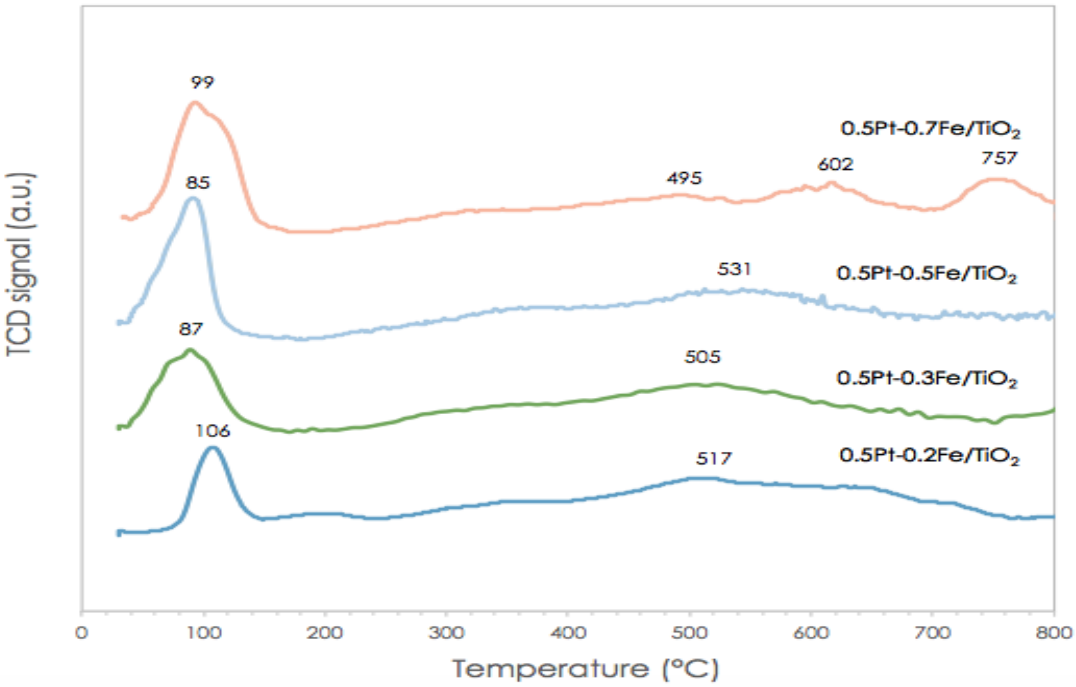

Figure 12. H_2 temperature-programmed reduction profiles of 0.5Pt-xFe/TiO_2 catalyst series.

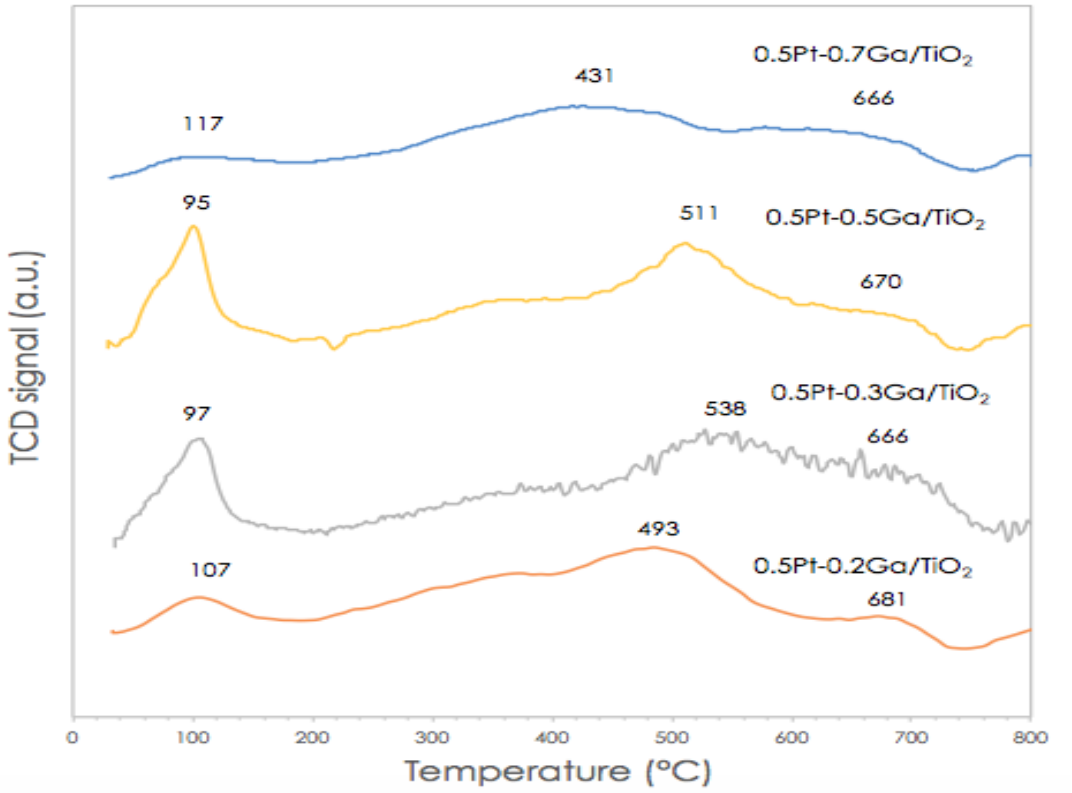

Figure 13 H_2 temperature-programmed reduction profiles of 0.5Pt-xGa/TiO_2 catalyst series.

4.2.1.4 N_2 physisorption

The BET surface area, pore volume, and pore diameter of the Pt based bimetallic catalyst are show in **Table 15.** There were significant decrease in the BET surface areas, average pore diameter, and pore volume upon second metal addition to the catalyst except that of 0.5Pt-0.5Fe/TiO_2 bimetallic catalyst which showed a significant decrease of BET surface area from 63 m^2/g to 19 m^2/g.

However, when considering the series of Pt-Fe bimetallic catalysts, the BET surface area and average pore diameter decreased monotonically with increasing of Fe metal loading from 0.2, 0.3, and 0.5 respectively.

Table 12. N_2 physisorption properties of Pt bimetallic catalyst/TiO_2

Catalysts	BET surface areas (m^2/g)	BJH pore diameter (nm)	BJH pore volume (cm^3/g)
0.5wt%Pt/TiO_2	63	18.45	0.37
0.5wt%Pt-0.2wt%Fe/TiO_2	56	17.16	0.30
0.5wt%Pt-0.3wt%Fe/TiO_2	48	15.80	0.23
0.5wt%Pt-0.5wt%Fe/TiO_2	19	13.33	0.30
0.5wt%Pt-0.7wt%Fe/TiO_2	58	13.63	0.26
0.5wt%Pt-0.2wt%Ga/TiO_2	55	15.85	0.29
0.5wt%Pt-0.5wt%Ni/TiO_2	47	19.13	0.30

Figure 14. illustrates the N_2 adsorption-desorption isotherms of Pt/TiO_2 and Pt based bimetallic catalysts. The catalyst exhibited type IV isotherm with a narrow and symmetrical hysteresis loops of type H1 at relative high-pressure range (P/P0), which connected to a narrow distribution of relatively uniform pores [23]. These results indicated the characteristics of mesoporous materials with pore diameter in the range of 2 to 50 nm.

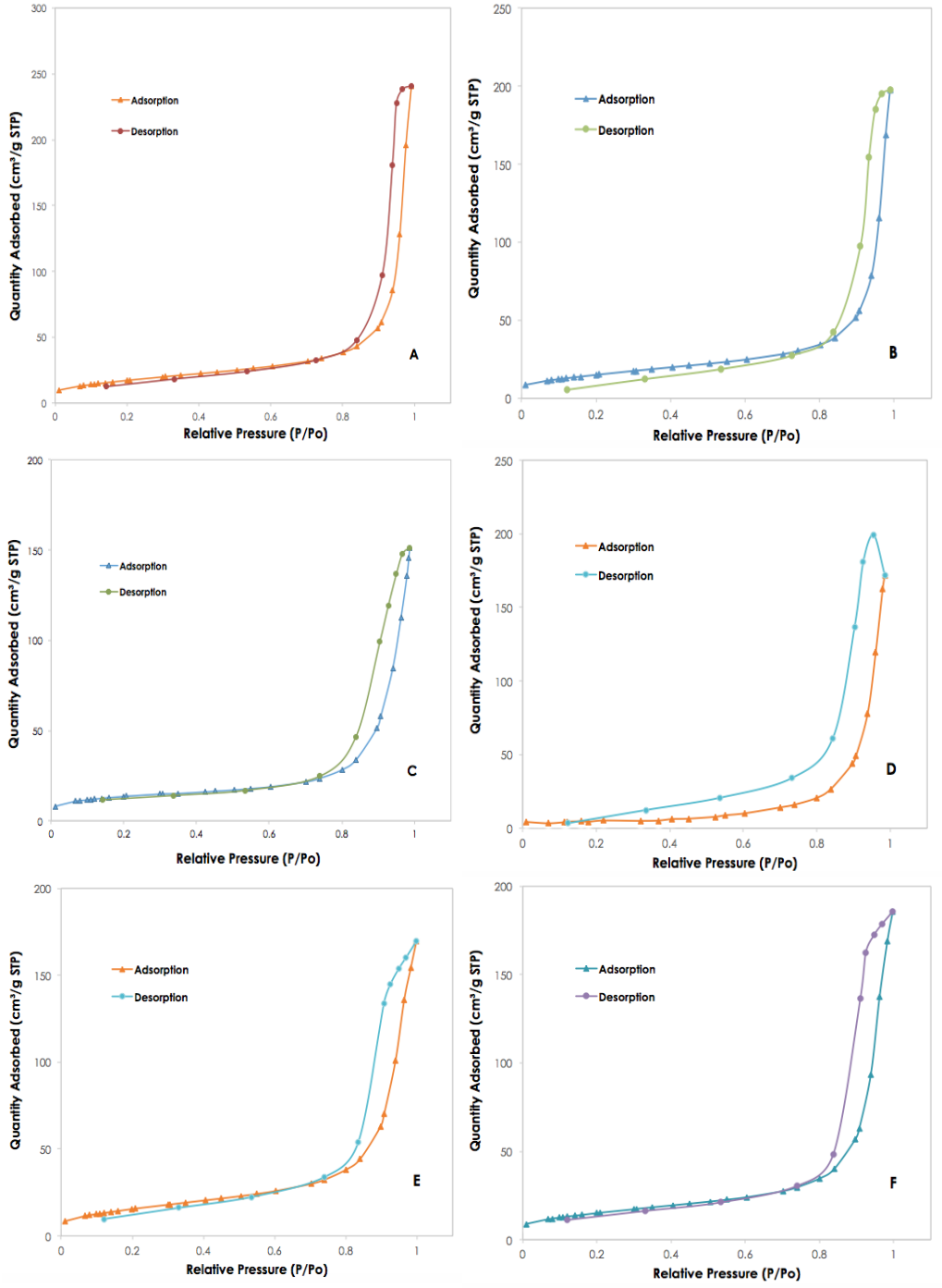

Figure 14. N_2 adsorption-desorption isotherm of Pt/TiO_2 and Pt based bimetallic catalyst/TiO_2 as a follow by $0.5Pt/TiO_2$ (A), $0.5Pt\text{-}0.2Fe/TiO_2$ (B), $0.5Pt\text{-}0.3Fe/TiO_2$ (C), $0.5Pt\text{-}0.5Fe/TiO_2$ (D), $0.5Pt\text{-}0.7Fe/TiO_2$ (E), and $0.5Pt\text{-}0.2Ga/TiO_2$ (F).

4.2.1.5 FTIR spectra of adsorbed CO

The FTIR spectra of adsorbed CO on the 0.5Pt/TiO_2 and 0.5Pt-xFe/TiO_2 catalysts with different Fe loadings are shown in **Figure 15,** the increase of Fe loading to 0.7wt% resulted in reducing of peak intensity of adsorbed CO on Pt sites on 0.5Pt-xFe/TiO_2 catalysts. On the 0.5Pt/TiO_2 catalyst, the spectrum unveiled the absorption band at 2058 cm^{-1}, revealing the demeanor of low-coordination Pt atoms on edge sites [24]. For 0.5Pt-0.7Fe/TiO_2 catalyst, the linear adsorption band at 2058 cm^{-1} was slightly shifted to 2073 cm^{-1} and bridge-coordinated CO species on Pt also shifted from 1826 cm^{-1} to 1840 cm^{-1} [25], thus, it might be because of the effect on the amount of Fe. Nevertheless, the adsorption band at 2092 cm^{-1}, that corresponded to the CO adsorbed on Pt terraces Pt(111) and Pt(100) were not significantly changed [6]. The adsorbed CO species on Fe was not detected in the CO adsorption spectra as a reported by Einaga H. et al. [22]. In addition, the figures of CO adsorption band on 0.5Pt-0.2Fe/TiO_2 and 0.5Pt-0.7Fe/TiO_2 were different from 0.5Pt/TiO_2. The CO-IR results were associated to the CO chemisorption results in which the 0.5Pt-0.2Fe/TiO_2 and 0.5Pt-0.7Fe/TiO_2 revealed much lower Pt active sites than the 0.5Pt/TiO_2.

It has been reported that bridge-type adsorbed CO formed mainly on large Pt particles, while linear-type adsorbed CO dominated on small Pt particles [4]. All of the catalysts unveiled the larger relative quantity of less-coordinated Pt atoms on edge, corner and kink sites. Such Pt sites were previously proposed by Corma A. et al. [26] to be the active sites for the selective hydrogenation of NS to VA. The author investigated the NS hydrogenation by using 0.2Pt/TiO_2 catalysts and measured FTIR spectra of adsorbed CO. Probably, the hydrogenation of the nitro group would preferentially proceed on such less-coordinated Pt sites as edge, corner, and kink, whereas that of the vinyl group would occur on the terrace sites.

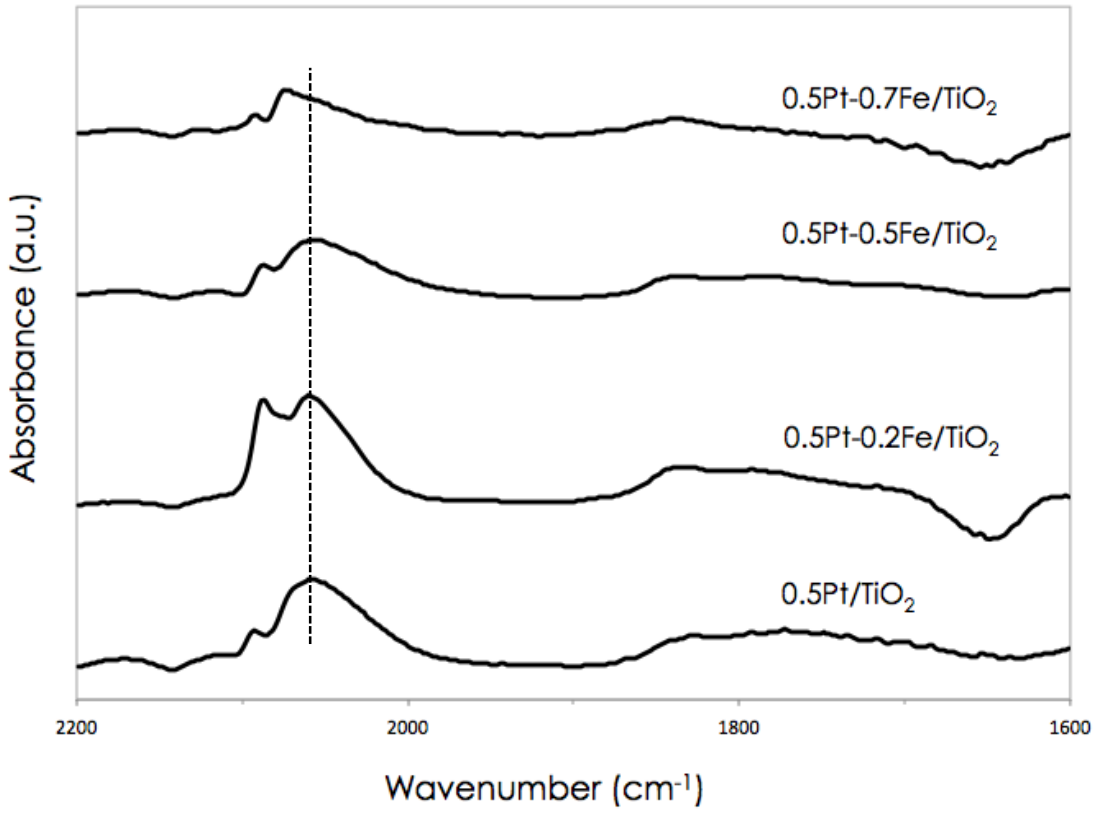

Figure 15 FTIR spectra of adsorbed CO over 0.5Pt /TiO_2 and 0.5Pt-xFe/TiO_2 catalysts.

4.2.1.6 XPS characterization

The oxidation state of platinum of 0.5Pt-xGa/TiO_2, 0.5Pt-xFe/TiO_2, and 0.5Pt-xCo/TiO_2 catalyst series was determined based on the fitted curve by XPS technique. **Figure 16.** displays the deconvolution of metallic Pt 4f signal on 0.5Pt-xGa/TiO_2 series in three species Pt^0, Pt^{+2}, and Pt^{+4} which allocated to Pt $4f_{7/2}$ level [27-29] and the last peak can be assigned to Pt $4f_{5/2}$ with Pt^{+4} species around 78.5-79.5 eV. When compare the peaks of all the catalysts in series, it is clearly seen that 0.5Pt-0.5Ga/TiO_2 and 0.5Pt-0.7Ga/TiO_2 had a low binding energy peak appeared nearby 68.8 eV and 69.5 eV, respectively. The peaks could be analogous to Pt-Ga alloy signals. Moreover, 0.5Pt-0.5Ga/TiO_2 catalyst has a broad signal around 75.6 eV but it did not have a signal around 78.5-79.5 eV which associated to Pt^{+4} species of Pt $4f_{5/2}$ [28].

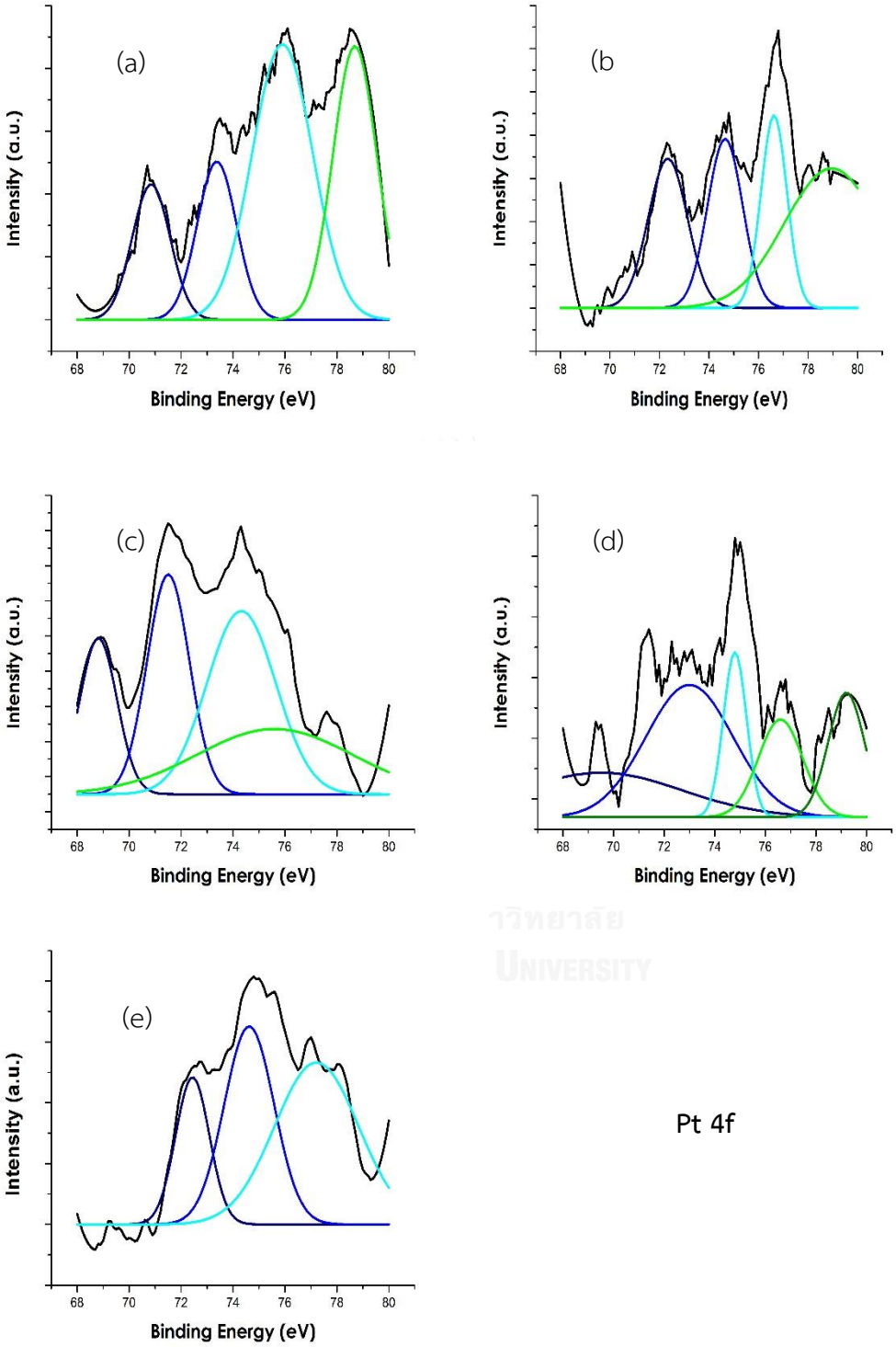

Figure 16. Pt XPS spectra of Pt 4f level for the 0.5Pt-xGa/TiO_2 catalyst series: (a) 0.5Pt-0.2Ga/TiO_2, (b) 0.5Pt-0.3Ga/TiO_2, (c) 0.5Pt-0.5Ga/TiO_2, (d) 0.5Pt-0.7Ga/TiO_2, and (e) 0.5Pt/TiO_2.

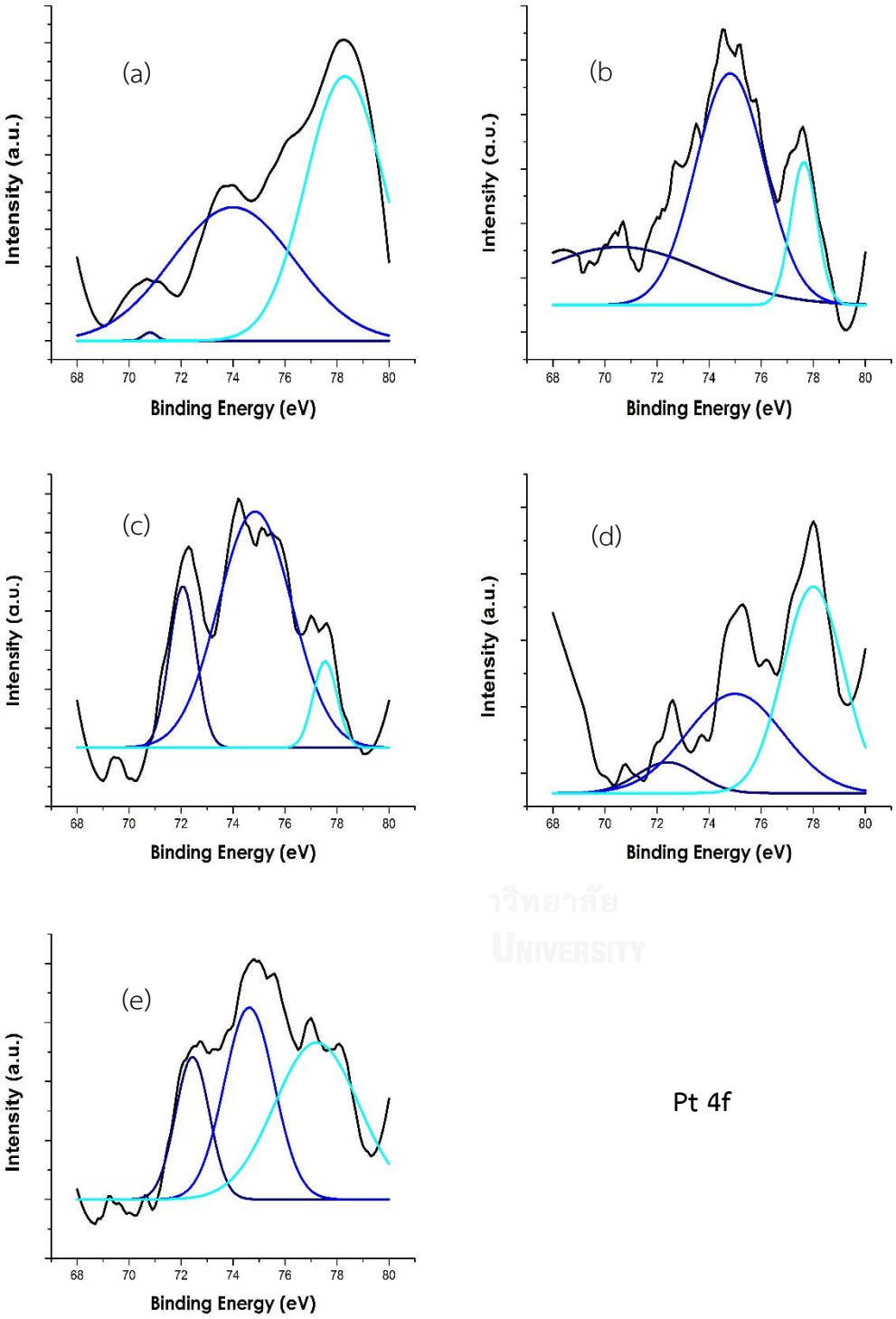

Figure 17. Pt XPS spectra of Pt 4f level for the 0.5Pt-xFe/TiO_2 catalyst series: (a) 0.5Pt-0.2Fe/TiO_2, (b) 0.5Pt-0.3Fe/TiO_2, (c) 0.5Pt-0.5Fe/TiO_2, (d) 0.5Pt-0.7Fe/TiO_2, and (e) 0.5Pt/TiO_2.

Table 13. XPS results for the 0.5Pt/TiO_2 catalyst, 0.5Pt-xGa/TiO_2, 0.5Pt-xGa/TiO_2, and 0.5Pt-xGa/TiO_2 catalyst series

Catalysts	Pt $4f_{7/2}$ level	
	BE (eV)	Species
0.5Pt/TiO_2	72.4	Pt^0
	74.6	Pt^{+2}
	77.2	Pt^{+4}
0.5Pt-0.2Ga/TiO_2	70.8	Pt^0
	73.4	Pt^{+2}
	75.9	Pt^{+4}
0.5Pt-0.3Ga/TiO_2	72.3	Pt^0
	74.6	Pt^{+2}
	76.6	Pt^{+4}
0.5Pt-0.5Ga/TiO_2	71.5	Pt^0
	74.3	Pt^{+2}
	75.6	Pt^{+4}
0.5Pt-0.7Ga/TiO_2	73.0	Pt^0
	74.8	Pt^{+2}
	76.6	Pt^{+4}
0.5Pt-0.2Fe/TiO_2	70.8	Pt^0
	74.0	Pt^{+2}
	78.3	Pt^{+4}
0.5Pt-0.3Fe/TiO_2	70.6	Pt^0
	74.8	Pt^{+2}
	77.6	Pt^{+4}
0.5Pt-0.5Fe/TiO_2	72.0	Pt^0
	74.8	Pt^{+2}
	77.5	Pt^{+4}
0.5Pt-0.7Fe/TiO_2	72.4	Pt^0

	75.0	Pt^{+2}
	78.0	Pt^{+4}
0.5Pt-0.2Co/TiO_2	72.5	Pt^{0}
	74.4	Pt^{+2}
	76.2	Pt^{+4}
0.5Pt-0.3Co/TiO_2	71.8	Pt^{0}
	74.8	Pt^{+2}
	76.0	Pt^{+4}
0.5Pt-0.5Co/TiO_2	72.8	Pt^{0}
	75.0	Pt^{+2}
	76.2	Pt^{+4}
0.5Pt-0.7Co/TiO_2	72.4	Pt^{0}
	74.6	Pt^{+2}
	76.3	Pt^{+4}

Stassi J.P. et al. has reported [28] Pt^{0} ~ 71-73 eV

Pt^{+2} ~ 73-75 eV

Pt^{+4} ~ 76-78 eV

Figure 17. unveil the Pt XPS **spectra** of 0.5Pt-xFe/TiO_2, the XPS spectra of metallic Pt 4f signal on 0.5Pt-xFe/TiO_2 series were consisted of 3 significant peaks that attributed to Pt $4f_{7/2}$ level (Pt^{0}, Pt^{+2}) and Pt $4f_{5/2}$ level, which illustrated binding energy around 70.5-71.5, 74-75, and 77-78.5 respectively. Besides, the Pt $4f_{7/2}$ signal of 0.5Pt-0.5Fe/TiO_2 and 0.5Pt-0.7Fe/TiO_2 were shifted to higher energy level from nearby 70.6-70.8 eV to 72.0-72.4 eV respectively, suggesting that Pt could form stable species by interacting with oxygenated groups that represent PtO due to increase amount of Fe and/or Pt-Fe alloy was formed [30]. The binding energy values (BE) of Pt $4f_{7/2}$ level, Pt species, and atomic % are shown in **Table 13**. The XPS Pt 4f signal of 0.5Pt-xCo/TiO_2 catalyst series were displayed in **Figure 18**, comparison of the peaks manifest that 0.5Pt-0.7Co/TiO_2 had the lowest signals compare to the other catalysts in series owing to the interaction between Pt with high amount of Co.

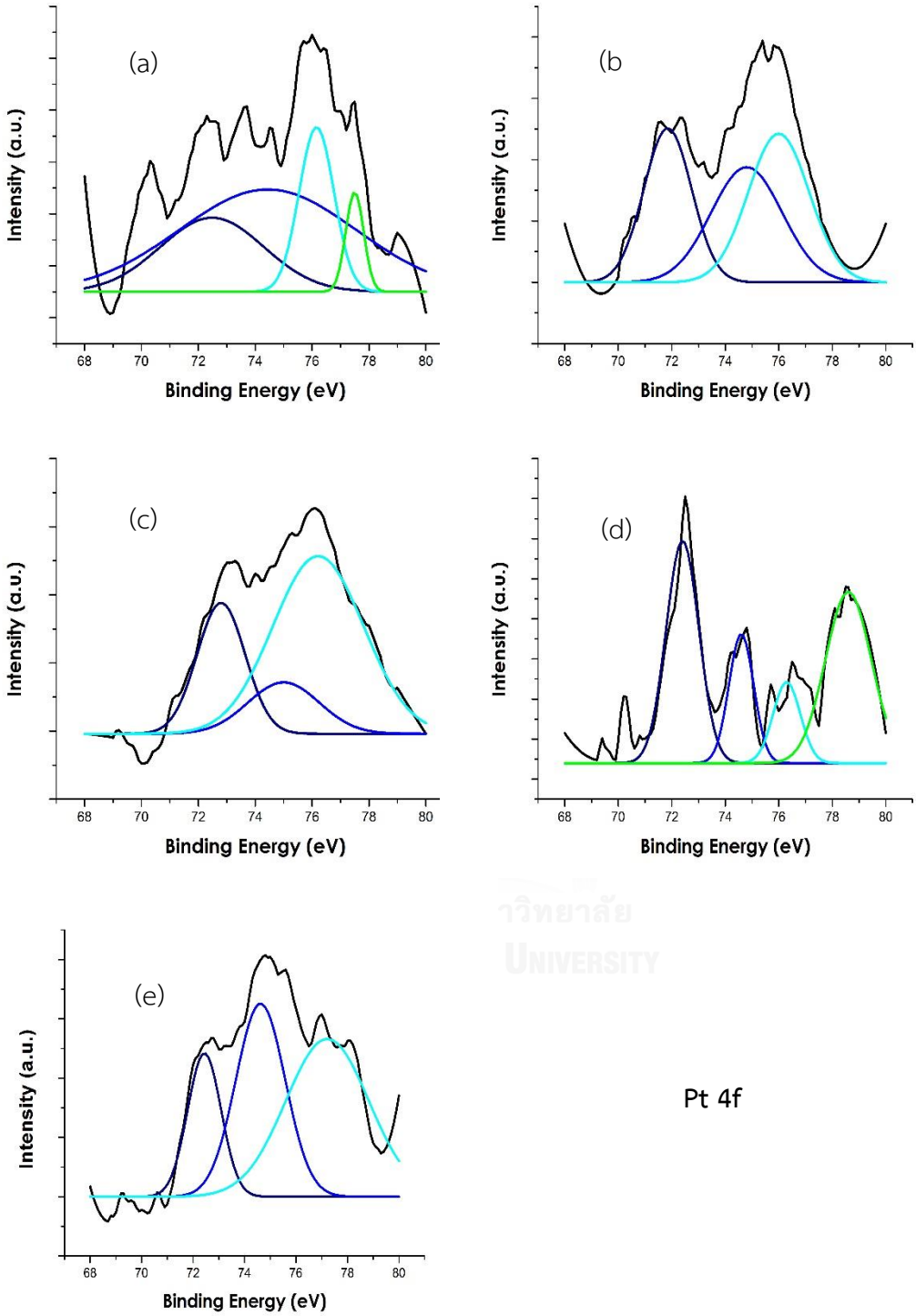

Figure 18 Pt XPS spectra of Pt 4f level for the 0.5Pt-xCo/TiO_2 catalyst series: (a) 0.5Pt-0.2Co/TiO_2, (b) 0.5Pt-0.3Co/TiO_2, (c) 0.5Pt-0.5Co/TiO_2, (d) 0.5Pt-0.7Co/TiO_2, and (e) 0.5Pt/TiO_2.

4.2.2 Catalytic activity

The catalytic performances of the 0.5Pt-0.2Co/TiO_2 and 0.5Pt-0.2Fe/TiO_2 catalysts for the liquid phase hydrogenation of 3-nitrostyrene at 50°C, 2 MPa, using 20 ml stainless steel autoclave reactor are illustrated in **Figure 19a and Figure 19b,** respectively. The hydrogenation of 3-nitrostyrene (3-NS) can occur through two reaction pathways from hydrogenation of the nitro group (N=O) and the vinyl group (C=C) followed by the formation of undesired hydrogenation products. The relationship between total conversion and product selectivity was acquired by using different reaction times. In this work, an improved catalytic performance in term of NS conversion was achieved over both catalysts. The conversion of 3-NS increased with increasing reaction times until complete conversion, but 3-vinylaniline (3-VA) selectivity decreased with times because of undesired hydrogenation occurred. However, the 0.5Pt-0.2Co/TiO_2 revealed the lowest 3-vinylaniline selectivity (10.1%) with 78.8% of 3-ethylaniline (3-EA) selectivity at reaction time 60 min. Similar results were also obtained in 0.5Pt-0.2Fe/TiO_2 catalyst that the 3-VA selectivity decreased from 89 to 68% during 150 min while the 3-EA selectivity increased from 8.1 to 31.3%. Moreover, these catalysts produced 3-ENB less than 1 % due to this catalyst tended to promote hydrogenation pathway of nitro group and then hydrogenate again to final product 3-EA. A yield of 3-VA on 0.5Pt-0.2Co/TiO_2 and 0.5Pt-0.2Fe/TiO_2 catalysts were displayed in **Figure 20**, the bar graph showed that the 0.5Pt-0.2Co/TiO_2 have fascinating catalytic activity but the yield of 3-VA fall off to 0.1 after 60 min. On the other hand, 0.5Pt-0.2Fe/TiO_2 showed slower catalytic activity with higher and more stable on 3-VA yield.

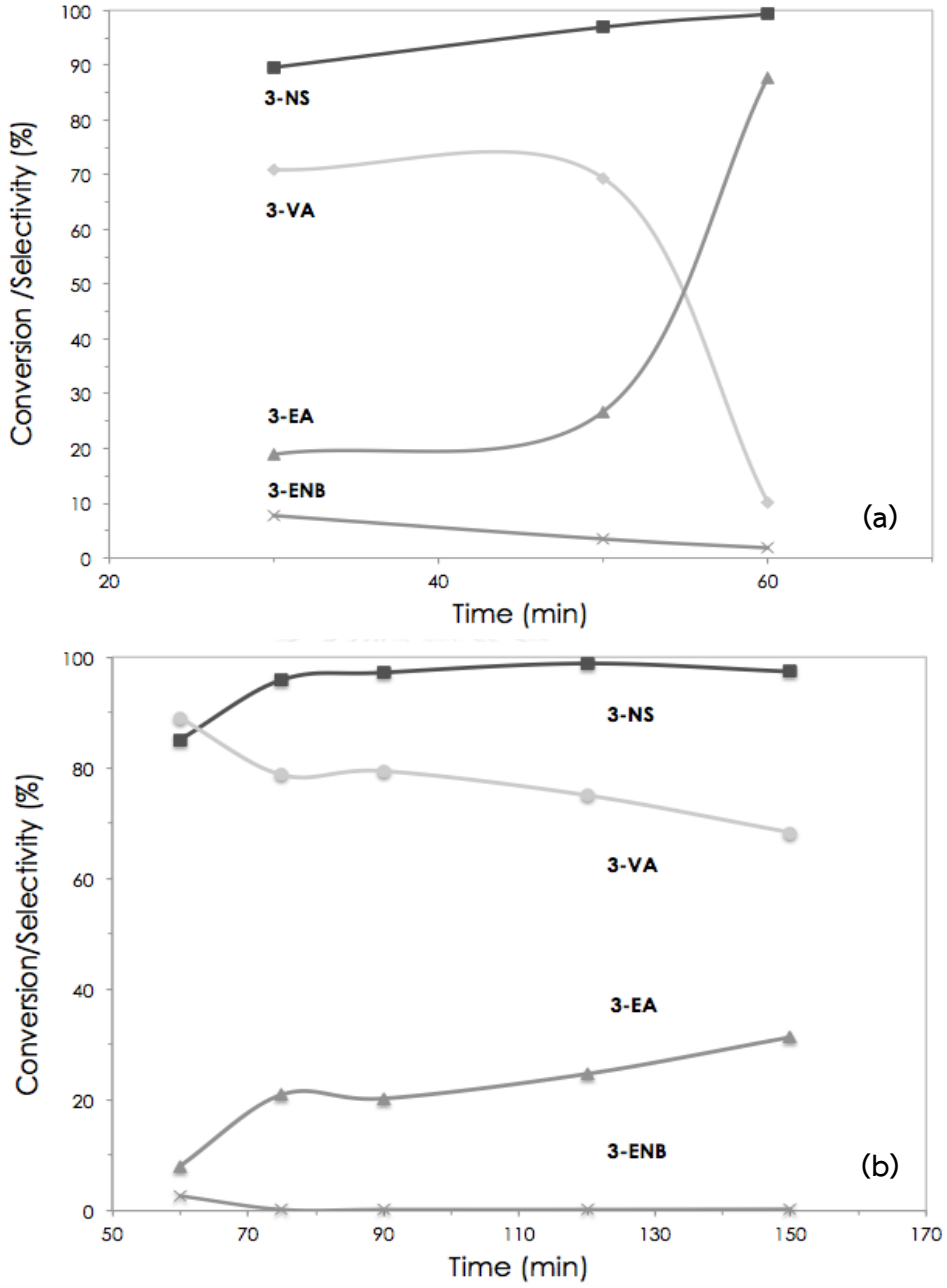

Figure 19. Result of 3-nitrostyrene hydrogenation in term of conversion and selectivity: (a) 0.5Pt-0.2Co/TiO_2 and (b) 0.5Pt-0.2Fe/TiO_2 catalysts.

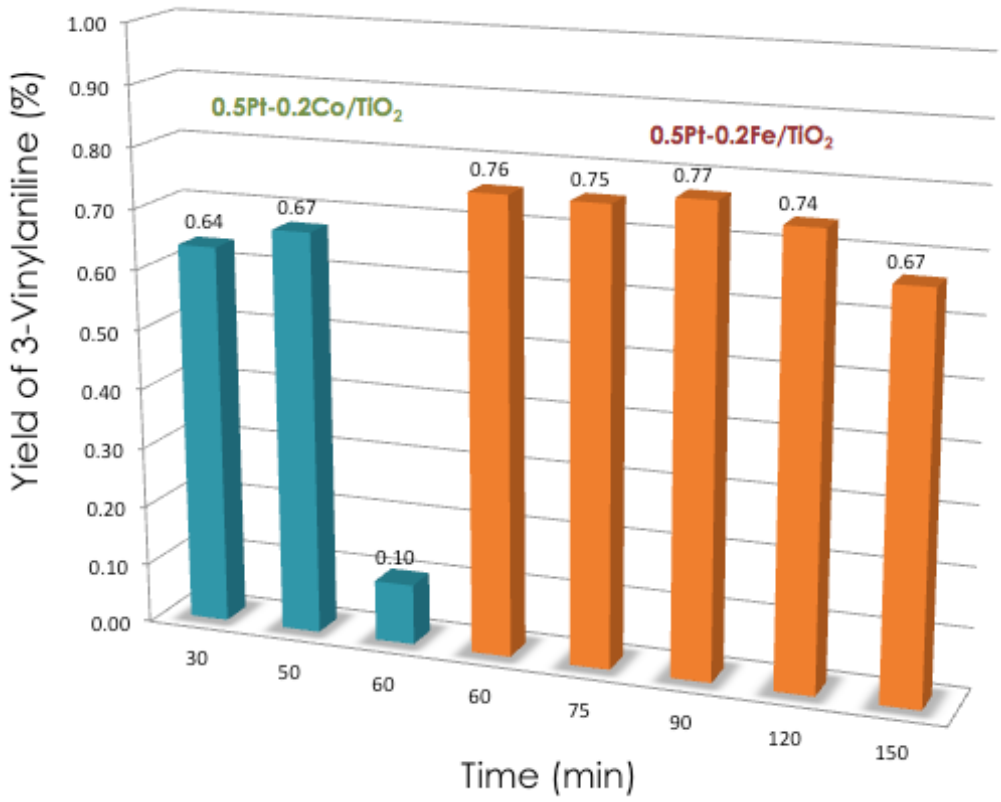

Figure 20. Yield of 3-vinylaniline on 0.5Pt-0.2Co/TiO_2 and 0.5Pt-0.2Fe/TiO_2 catalysts with different reaction time.

Table 16. Conversion and product selectivity for 3-nitrostyene hydrogenation over 0.5Pt-xGa/TiO_2 bimetallic catalyst series (Reaction conditions: 2MPa of H_2 gas, 50°C, 20 mg of reduced catalyst, 10 mL of ethanol, and 1 h batch.).

Catalyst	NS conversion (%)	Selectivity (%)			
		VA	ENB	EA	Intermediate
0.5Pt/TiO_2	67.7	57.6	24.9	14.5	3.0
0.5Pt-0.2Ga/TiO_2	89.7	80.8	4.8	13.5	0.9
0.5Pt-0.3Ga/TiO_2	98.6	68.2	1.9	29.8	0.1
0.5Pt-0.5Ga/TiO_2	68.6	65.2	17.9	14.6	2.3
0.5Pt-0.7Ga/TiO_2	42.7	71.5	16.2	6.8	5.5

Table 17. Conversion and product selectivity for 3-nitrostyene hydrogenation over 0.5Pt-xFe/TiO_2 bimetallic catalyst series *(Reaction conditions: 2MPa of H_2 gas, 50°C, 20 mg of reduced catalyst, 10 mL of ethanol, and 1 h batch.).*

Catalyst	NS conversion (%)	Selectivity (%)			
		VA	ENB	EA	Intermediate
0.5Pt/TiO_2	67.7	57.6	24.9	14.5	3.0
0.5Pt-0.2Fe/TiO_2	89.7	85.1	2.7	8.0	0.3
0.5Pt-0.3Fe/TiO_2	98.6	98.9	1.0	23.8	0.0
0.5Pt-0.5Fe/TiO_2	68.6	81.3	0.2	18.4	0.1
0.5Pt-0.7Fe/TiO_2	42.7	79.0	8.9	12.0	0.1

Table 18. Conversion and product selectivity for 3-nitrostyene hydrogenation over 0.5Pt-xCo/TiO_2 bimetallic catalyst series *(Reaction conditions: 2MPa of H_2 gas, 50°C, 20 mg of reduced catalyst, 10 mL of ethanol, and 1 h batch.).*

Catalyst	NS conversion (%)	Selectivity (%)			
		VA	ENB	EA	Intermediate
0.5Pt/TiO_2	67.7	57.6	24.9	14.5	3.0
0.5Pt-0.2Co/TiO_2	99.3	10.1	1.8	87.8	0.3
0.5Pt-0.3Co/TiO_2	82.7	64.1	14.1	20.6	1.2
0.5Pt-0.5Co/TiO_2	77.4	60.0	18.4	15.6	6.0
0.5Pt-0.7Co/TiO_2	39.4	62.4	23.1	9.8	4.7

Furthermore, the catalytic activity of 0.5Pt-xGa/TiO_2, 0.5Pt-xFe/TiO_2, and 0.5Pt-xCo/TiO_2 series were also examined in the liquid phase hydrogenation of 3-nitrostyrene at 50°C, 2 MPa, reaction time 1 h, and using 20 ml stainless steel autoclave reactor. **Figure 21** presents the results of 3-nitrostyrene conversion with different amounts of second metal varying from 0.2 to 0.7 weight %. According to the results, both of 0.5Pt-xCo/TiO_2 and 0.5Pt-xGa/TiO_2 catalyst series exhibited relatively low NS conversion when deposited more amount of second metal on the catalysts. On the other hand, for the 0.5Pt-xFe/TiO_2 series superior NS conversion was obtained, perhaps, because of interaction between Pt-Fe that led to the promotion of 3-nitrostyrene conversions and/or Pt-Fe alloy form had more favor to attract H_2 in NS.

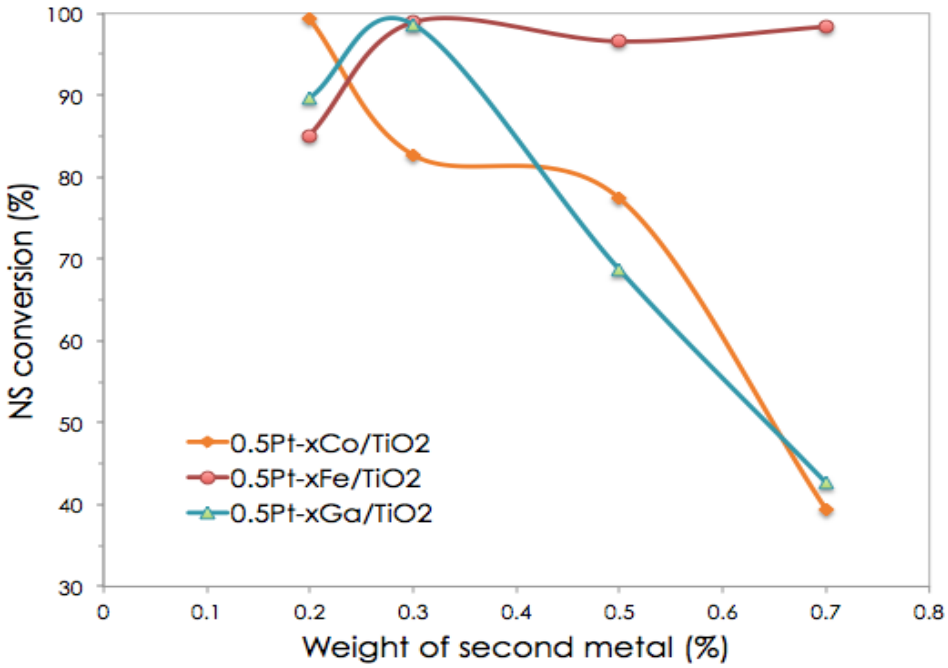

Figure 21. Result of 3-nitrostyrene hydrogenation in term of conversion with different Pt based bimetallic catalyst series *(Reaction conditions: 2MPa of H_2 gas, 50°C, 20 mg of reduced catalyst, 10 mL of ethanol, and 1 h batch.).*

Additional results can be seen from **Figure 22.**only 0.5Pt-xFe/TiO_2 catalyst series indicated in high piority of VA selectivity and NS conversion. It was rationalized that the presence of Fe second metal in the Pt/TiO_2 catalyst could be reliable for the increase selectivity to vinylaniline and nitrostyrene conversion.

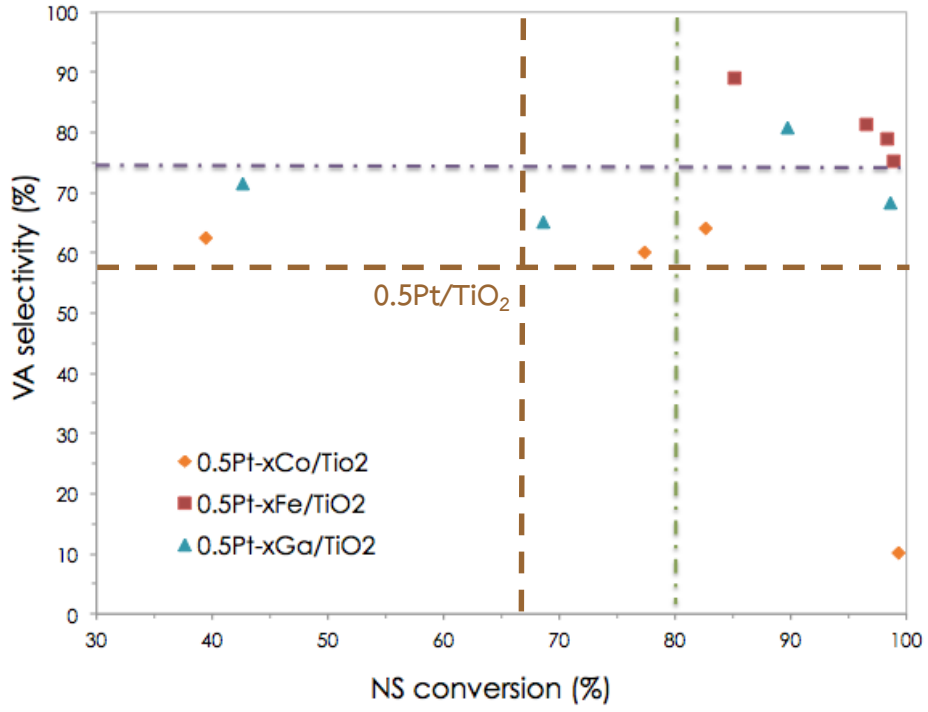

Figure 22. Hydrogenation of 3-nitrostyrene on 0.5Pt-xCo/TiO_2, 0.5Pt-xFe/TiO_2, and 0.5Pt-xGa/TiO_2 series *(Reaction conditions: 2MPa of H_2 gas, 50°C, 20 mg of reduced catalyst, 10 mL of ethanol, and 1 h batch.).*

In summary, the 0.5Pt-xFe/TiO_2 series exhibited the highest yield of 3-VA between 0.74 to 0.78 when compared to the other catalyst series as shown in **Figure 23.** It is suggested that the 0.5Pt-xFe/TiO_2 catalyst series were the most effective Pt based bimetallic catalysts for the liquid phase hydrogenation of 3-nitrostyrene. When comparing among the 0.5Pt-xFe/TiO_2 catalysts, the 0.5Pt-0.5Fe/TiO_2 catalyst was the best catalyst according to the CO Chemisorption results and the catalytic results because it gave really low 3-ENB 0.22% at nearly complete conversion.

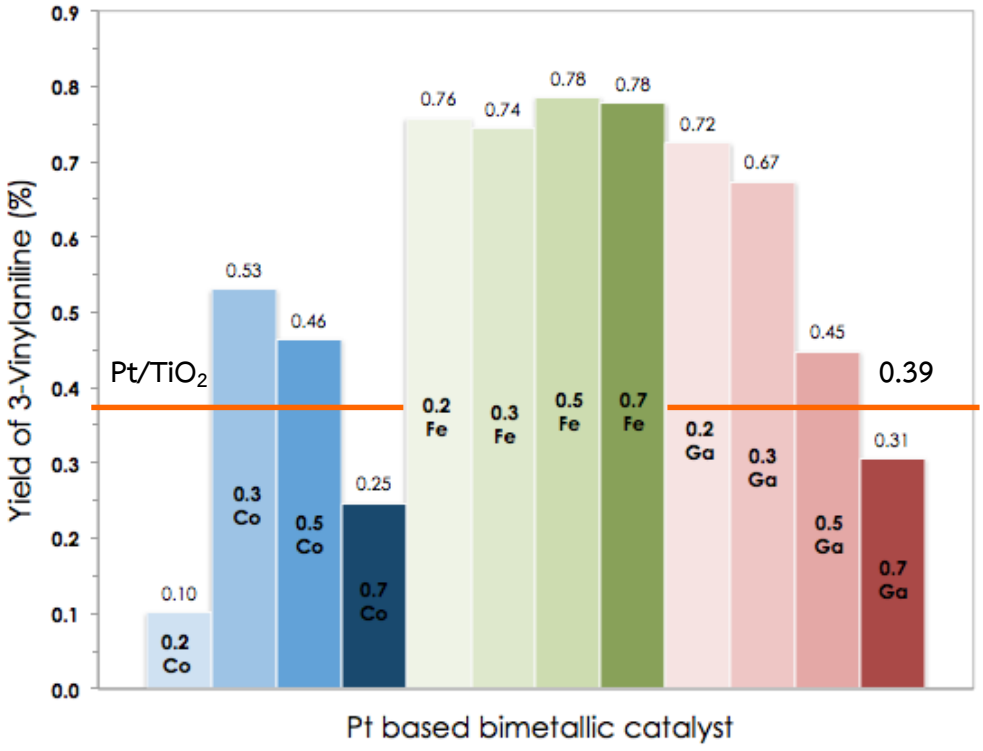

Figure 23. Yield of 3-vinylaniline on Pt based bimetallic catalysts *(Reaction conditions: 2MPa of H_2 gas, 50°C, 20 mg of reduced catalyst, 10 mL of ethanol, and 1 h batch.).*

CHAPTER 5

CONCLUSIONS AND RECOMMENDATIONS

The effects of the second metal and the amounts of second metal on the Pt based bimetallic catalyst were investigated in the liquid phase selective hydrogenation of 3-nitrostyrene to 3-vinylaniline. The conclusions and recommendations are given redundant.

5.1 Conclusions

The catalytic screening test of Pt based bimetallic catalysts with Cr, Ni, Cu, Zn, Co, Fe, and Ga, found that only 0.5Pt-0.5Co/TiO_2, 0.5Pt-0.5Fe/TiO_2, and 0.5Pt-0.5Ga/TiO_2 gave good performance compared to Pt monometallic catalyst. The dispersion and active site of Pt catalyst were decreased when the 2nd metal presented, the same way in H_2-TPR, the reduction peaks of Pt oxide shifted to lower temperature.

From the catalytic results, addition of an appropriate amount of a second metal (Co, Fe, or Ga) to Pt/TiO_2 led to an improved catalytic performance in the hydrogenation of 3-NS, the conversion of 3-NS increased with increasing reaction times until complete conversion. In particular, the 0.5Pt-0.2Co/TiO_2 catalyst has highest catalytic activity because they gave 90% of NS conversion in 30 min compared to 0.5Pt-0.2Fe/TiO_2. Moreover, I was found that the 0.5Pt-xFe/TiO_2 series exhibited superior NS conversion and higher 3-VA selectivity than the monometallic Pt catalyst. The Pt-Co(0.3-0.5%) and Pt-Ga(0.2-0.5%) also showed improved catalytic performances. The activity of the bimetallic Pt-based catalysts did not follow the CO-chemisorption trend due probably to the Pt-alloy formation and/or the coverage of Pt active site by the 2nd metal. However, the H_2-TPR results showed that the reducibility of Pt oxide was easier for the bimetallic catalysts and the XRD results revealed the presence of amorphous phase when Fe, Co, or Ga were added to the Pt catalysts. This could be the reason for higher VA selectivity of these catalysts.

On the contrary, the 0.5Pt-xFe/TiO_2 catalyst series unveiled highest selectivity to 3-VA perhaps, because of interaction between Pt-Fe raise the hydrogenation of nitro group instead of vinyl group, and/or Pt-Fe alloy form had more favor to attract H_2 in NS. When comparing among the 0.5Pt-xFe/TiO_2 catalysts, the 0.5Pt-0.5Fe/TiO_2 was the best catalyst performances which gave the lowest undesired product (3-ethylnitrobenzene) about 0.2 % with highest yield of 3-VA at 78%.

5.2 Recommendations

1. Study the alloy formation of Pt-base bimetallic catalyst at different calcination temperature, it's fascinated because calcination temperature is a major factor of alloy formation.

2. Investigate the effect of alloy formation of Pt-base bimetallic catalyst on electronic properties and catalytic reaction because this is a one of the reasons that influence the catalytic performance.

REFERENCES

1. Fujita, S.-i., et al., *Selective hydrogenation of nitrostyrene to aminostyrene over Pt/TiO2 catalysts: Effects of pressurized carbon dioxide and catalyst preparation conditions.* The Journal of Supercritical Fluids, 2011. **60**: p. 106-112.
2. Serna, P., M. Boronat, and A. Corma, *Tuning the Behavior of Au and Pt Catalysts for the Chemoselective Hydrogenation of Nitroaromatic Compounds.* Topics in Catalysis, 2011. **54**(5): p. 439-446.
3. Furukawa, S., Y. Yoshida, and T. Komatsu, *Chemoselective Hydrogenation of Nitrostyrene to Aminostyrene over Pd- and Rh-Based Intermetallic Compounds.* ACS Catalysis, 2014. **4**(5): p. 1441-1450.
4. Boronat, M., et al., *A Molecular Mechanism for the Chemoselective Hydrogenation of Substituted Nitroaromatics with Nanoparticles of Gold on TiO2 Catalysts: A Cooperative Effect between Gold and the Support.* Journal of the American Chemical Society, 2007. **129**(51): p. 16230-16237.
5. Makosch, M., et al., *Organic Thiol Modified Pt/TiO2 Catalysts to Control Chemoselective Hydrogenation of Substituted Nitroarenes.* ACS Catalysis, 2012. **2**(10): p. 2079-2081.
6. Pisduangdaw, S., et al., *Flame-made Pt/TiO2 catalysts for the liquid-phase selective hydrogenation of 3-nitrostyrene.* Applied Catalysis A: General, 2015. **490**: p. 193-200.
7. Serna, P., P. Concepción, and A. Corma, *Design of highly active and chemoselective bimetallic gold–platinum hydrogenation catalysts through kinetic and isotopic studies.* Journal of Catalysis, 2009. **265**(1): p. 19-25.
8. Yu, W., M.D. Porosoff, and J.G. Chen, *Review of Pt-Based Bimetallic Catalysis: From Model Surfaces to Supported Catalysts.* Chemical Reviews, 2012. **112**(11): p. 5780-5817.

9. Landmann, M., E. Rauls, and W.G. Schmidt, *The electronic structure and optical response of rutile, anatase and brookite TiO 2.* Journal of Physics: Condensed Matter, 2012. **24**(19): p. 195503.
10. Hu, Y., H.L. Tsai, and C.L. Huang, *Phase transformation of precipitated TiO2 nanoparticles.* Materials Science and Engineering: A, 2003. **344**(1–2): p. 209-214.
11. Wetchakun, N. and S. Phanichphant, *Effect of temperature on the degree of anatase–rutile transformation in titanium dioxide nanoparticles synthesized by the modified sol–gel method.* Current Applied Physics, 2008. **8**(3–4): p. 343-346.
12. Bally, A., *Electronic properties of nano-crystalline titanium dioxide thin films*. 1999, EPFL.
13. Pisduangdaw, S., et al., *One step synthesis of Pt–Co/TiO2 catalysts by flame spray pyrolysis for the hydrogenation of 3-nitrostyrene.* Catalysis Communications, 2015. **61**: p. 11-15.
14. Campbell, C.T., *Bimetallic Surface Chemistry.* Annual Review of Physical Chemistry, 1990. **41**(1): p. 775-837.
15. Rodriguez, J., *Physical and chemical properties of bimetallic surfaces.* Surface Science Reports, 1996. **24**(7): p. 223-287.
16. Chen, J.G., C.A. Menning, and M.B. Zellner, *Monolayer bimetallic surfaces: Experimental and theoretical studies of trends in electronic and chemical properties.* Surface Science Reports, 2008. **63**(5): p. 201-254.
17. Beier, M.J., J.-M. Andanson, and A. Baiker, *Tuning the Chemoselective Hydrogenation of Nitrostyrenes Catalyzed by Ionic Liquid-Supported Platinum Nanoparticles.* ACS Catalysis, 2012. **2**(12): p. 2587-2595.
18. Li, X., et al., *Porous TiO2 Materials through Pickering High-Internal Phase Emulsion Templating.* Langmuir, 2014. **30**(10): p. 2676-2683.
19. Zhang, Y., et al., *TiO2–Graphene Nanocomposites for Gas-Phase Photocatalytic Degradation of Volatile Aromatic Pollutant: Is TiO2–Graphene Truly Different from Other TiO2–Carbon Composite Materials?* ACS Nano, 2010. **4**(12): p. 7303-7314.

20. Panpranot, J., K. Kontapakdee, and P. Praserthdam, *Effect of TiO2 Crystalline Phase Composition on the Physicochemical and Catalytic Properties of Pd/TiO2 in Selective Acetylene Hydrogenation.* The Journal of Physical Chemistry B, 2006. **110**(15): p. 8019-8024.
21. Pongthawornsakun, B., et al., *Effect of reduction temperature on the characteristics and catalytic properties of TiO2 supported AuPd alloy particles prepared by one-step flame spray pyrolysis in the selective hydrogenation of 1-heptyne.* Applied Catalysis A: General, 2015. **506**: p. 278-287.
22. Einaga, H., et al., *CO Oxidation Over TiO2-Supported Pt–Fe Catalysts Prepared by Coimpregnation Methods.* Catalysis Letters, 2014. **144**(10): p. 1653-1660.
23. Riyapan, S., et al., *Improved catalytic performance of Pd/TiO2 in the selective hydrogenation of acetylene by using H2-treated sol–gel TiO2.* Journal of Molecular Catalysis A: Chemical, 2014. **383–384**: p. 182-187.
24. Raskó, J., *CO-induced surface structural changes of Pt on oxide-supported Pt catalysts studied by DRIFTS.* Journal of Catalysis, 2003. **217**(2): p. 478-486.
25. Soares, A.V.-H., G. Perez, and F.B. Passos, *Alumina supported bimetallic Pt–Fe catalysts applied to glycerol hydrogenolysis and aqueous phase reforming.* Applied Catalysis B: Environmental, 2016. **185**: p. 77-87.
26. Corma, A., et al., *Transforming Nonselective into Chemoselective Metal Catalysts for the Hydrogenation of Substituted Nitroaromatics.* Journal of the American Chemical Society, 2008. **130**(27): p. 8748-8753.
27. Shukla, A.K., et al., *An XPS study on binary and ternary alloys of transition metals with platinized carbon and its bearing upon oxygen electroreduction in direct methanol fuel cells.* Journal of Electroanalytical Chemistry, 2001. **504**(1): p. 111-119.
28. Stassi, J.P., et al., *Ga and In promoters in bimetallic Pt based catalysts to improve the performance in the selective hydrogenation of citral.* Applied Catalysis A: General, 2015. **497**: p. 58-71.

29. Wu, Z., et al., *Deactivation mechanism of PtOx/TiO2 photocatalyst towards the oxidation of NO in gas phase.* Journal of Hazardous Materials, 2011. **185**(2–3): p. 1053-1058.

30. Berguerand, C., et al., *Chemoselective Liquid Phase Hydrogenation of 3-Nitrostyrene over Pt Nanoparticles: Synergy with ZnO Support.* Industrial & Engineering Chemistry Research, 2015. **54**(35): p. 8659-8669.

APPENDIX

Appendix A

Calculation for all Pt-based bimetallic catalysts preparation

A.1 The preparation of 0.5 wt% Pt based bimetallic catalyst overed TiO_2 (Degussa P25) by CO-Incipient wetness impregnation method

Example calculation for the preparation of 0.5wt%Pt-0.5wt%Fe/TiO_2

Data Calculation :

-Chloroplatinic acid hexahydrate 37.5% ($H_2PtCl_6 \cdot 6H_2O$) , MW = 517.90 g/mol

-Pt, MW = 195.08 g/mol

-Iron(III) nitrate nonahydrate ($Fe(NO_3)_3 \cdot 9H_2O$) = 404.00 g/mol

-Fe, MW = 55.85 g/mol

-TiO_2 (Degussa P25) = 79.87 g/mol

Calculation based on the composition of the catalyst and weight 100 g of catalyst was follows by Platinum = 0.5 g and Fe = 0.5 g (Pt:Fe = 1:1)

Then, TiO_2 = 100 – Pt - Fe = 100-0.5-0.5 = 99.0 g

If we used TiO_2 1 g Then, Platinum required = $\frac{(1g)x(0.5g\ Pt)}{(99.0g)}$ = 5.05 x 10^{-3} g

Platinum 5.05 x 10^{-3} g was perpared from $H_2PtCl_6 \cdot 6H_2O$

Then, $H_2PtCl_6 \cdot 6H_2O$ required = $\frac{\mathbf{MW\ of\ (H_2PtCl_6 \cdot 6H_2O)\ x\ Pt\ required}}{\mathbf{MW\ of\ Pt}}$

$= \frac{(517.90\ g/mol\ )x(5.05\ x\ 10^{-3}\ g\ )}{(195.08\ g/mol)}$

So, $H_2PtCl_6 \cdot 6H_2O$ required = 0.0134 g

The same way,

If we used TiO_2 1 g Then, Iron required = $\frac{(1g)x(0.5g\ Fe)}{(99.0g)}$ = 5.05 x 10^{-3} g

Iron 5.05 x 10^{-3} g was perpared from $Fe(NO_3)_3 \cdot 9H_2O$

Then, $Fe(NO_3)_3 \cdot 9H_2O$ required = $\frac{\text{MW of } (Fe(NO_3)_3 \cdot 9H_2O) \text{ x Fe required}}{\text{MW of Fe}}$

$$= \frac{(404.00\ g/mol\ )x(5.05\ x\ 10^{-3}\ g\ )}{(55.85\ g/mol)}$$

So, $Fe(NO_3)_3 \cdot 9H_2O$ required = 0.0365 g

A.2 The preparation of 0.5 wt% Pt based bimetallic catalyst with different second metal loading overed TiO_2 (Degussa P25)

Example calculation for the preparation of 0.5wt%Pt-0.2wt%Co/TiO_2

Data Calculation :

-Chloroplatinic acid hexahydrate 37.5% ($H_2PtCl_6 \cdot 6H_2O$) , MW = 517.90 g/mol

-Pt, MW = 195.08 g/mol

-Cobalt(II) nitrate hexahydrate ($Co(NO_3)_2 \cdot 6H_2O$)= 291.03 g/mol

-Co, MW = 58.93 g/mol

-TiO_2 (Degussa P25) = 79.87 g/mol

Calculation based on the composition of the catalyst and weight 100 g of catalyst

was follows by Platinum = 0.5 g and Co = 0.2 g (Pt:Co = 5:2)

Then, TiO_2 = 100 – Pt - Co = 100-0.5-0.2 = 99.3 g

If we used TiO_2 1 g Then, Platinum required = $\frac{(1g)x(0.5g\ Pt)}{(99.3g)}$ = 5.04 x 10^{-3} g

Platinum 5.04 x 10^{-3} g was perpared from $H_2PtCl_6 \cdot 6H_2O$

Then, $H_2PtCl_6 \cdot 6H_2O$ required = $\frac{MW\ of\ (H_2PtCl_6 \cdot 6H_2O)\ x\ Pt\ required}{MW\ of\ Pt}$

$$= \frac{(517.90\ g/mol\ )x(5.04\ x\ 10^{-3}\ g\ )}{(195.08\ g/mol)}$$

So, $H_2PtCl_6 \cdot 6H_2O$ required = 0.0134 g

The same way,

If we used TiO_2 1 g Then, Cobalt required = $\frac{(1g)x(0.2g\ Co)}{(99.3g)}$ = 2.01 x 10^{-3} g

Cobalt 2.01 x 10^{-3} g was perpared from $Co(NO_3)_2 \cdot 6H_2O$

Then, $Co(NO_3)_2 \cdot 6H_2O$ required = $\frac{MW\ of\ (Co(NO_3)_2 \cdot 6H_2O)\ x\ Co\ required}{MW\ of\ Co}$

$$= \frac{(291.03g/mol)x(2.01\ x\ 10^{-3}\ g\ )}{(58.93\ g/mol)}$$

So, $Co(NO_3)_2 \cdot 6H_2O$ required = 0.0099 g

Appendix B

Calculation of all CO-Chemisorption

Calculation of the amount of Pt active sites and the % dispersion, which a stoichiometry of CO/Pt = 1(Sf=1), measured by CO chemisorption is as follows:

The weight of catalyst used	=	W	g
Loop volume dosed	=	V_{loop}	μL
Integral area of CO peak after adsorption	=	Ai	unit
Integral area of 20 μL of standard CO peak	=	Af	unit
Molar volume of gas at STP (Vg)	=	22414	cm^3/mol
% Metal used	=	%M	%
Molecular weight of the metal	=	MW	a.m.u.
Avogadro's number	=	$6.023x10^{23}$	molecules/mol
Stoichiometry factor	=	Sf	
Amount of CO adsorbed on catalyst	=	$\frac{\mathbf{Vloop x} \sum(\boldsymbol{Af-Ai})}{\boldsymbol{W-Af}}$	= A μL/gcat
Amount of CO adsorbed on catalyst (Vads)	=	A/1000	= B cm^3/gcat
Molecule of CO adsorbed on catalyst	= Metal active site		
	= Sf x $\frac{\boldsymbol{Vads}}{\boldsymbol{Vg}}$ x$6.023x10^{23}$molecules/g.cat		
%Dispersion	= Sf x $\frac{\boldsymbol{Vads}}{\boldsymbol{Vg}}$ x $\frac{\boldsymbol{m.w.}}{\%\boldsymbol{M}}$ x100% x100%		

Appendix C

XPS data of Pt based bimetallic catalyst series

The data table of elemental % on surface of Pt based bimetallic catalyst series

C.1 The data table of elemental % on surface of 0.5Pt-xCo/TiO_2 catalyst series

Catalyst	Pt		Co		Ti		O	
	Atom%	Wt%	Atom%	Wt%	Atom%	Wt%	Atom%	Wt%
0.5Pt/TiO_2	0.12	0.84	-	-	27.65	52.94	72.23	46.22
0.5Pt-0.2Co/TiO_2	0.38	2.82	6.29	13.93	22.82	40.95	70.51	42.30
0.5Pt-0.3Co/TiO_2	0.33	2.45	4.77	10.78	23.15	42.63	71.75	44.14
0.5Pt-0.5Co/TiO_2	0.15	1.16	1.44	3.52	22.89	45.35	75.50	49.99
0.5Pt-0.7Co/TiO_2	0.24	1.94	4.74	11.11	20.77	39.64	74.25	47.31

C.2 The data table of elemental % on surface of 0.5Pt-xFe/TiO_2 catalyst series

Catalyst	Pt		Fe		Ti		O	
	Atom%	Wt%	Atom%	Wt%	Atom%	Wt%	Atom%	Wt%
0.5Pt/TiO_2	0.12	0.84	-	-	27.65	52.94	72.23	46.22
0.5Pt-0.2Fe/TiO_2	0.44	3.16	7.56	15.60	23.03	40.60	68.97	40.64
0.5Pt-0.3Fe/TiO_2	0.40	3.13	4.12	9.24	20.58	39.55	74.90	48.08
0.5Pt-0.5Fe/TiO_2	0.12	0.88	1.53	3.48	24.26	47.34	74.09	48.30
0.5Pt-0.7Fe/TiO_2	0.28	2.49	2.67	6.65	23.61	43.76	73.44	47.09

C.3 The data table of elemental % on surface of 0.5Pt-xGa/TiO_2 catalyst series

Catalyst	Pt		Ga		Ti		O	
	Atom%	Wt%	Atom%	Wt%	Atom%	Wt%	Atom%	Wt%
0.5Pt/TiO_2	0.12	0.84	-	-	27.65	52.94	72.23	46.22
0.5Pt-0.2Ga/TiO_2	-	-	-	-	-	-	-	-
0.5Pt-0.3Ga/TiO_2	-	-	-	-	-	-	-	-
0.5Pt-0.5Ga/TiO_2	0.14	1.01	3.17	8.43	26.13	47.59	70.56	42.97
0.5Pt-0.7Ga/TiO_2	-	-	-	-	-	-	-	-

The XPS spectra of Pt based bimetallic series with different 2nd metal level

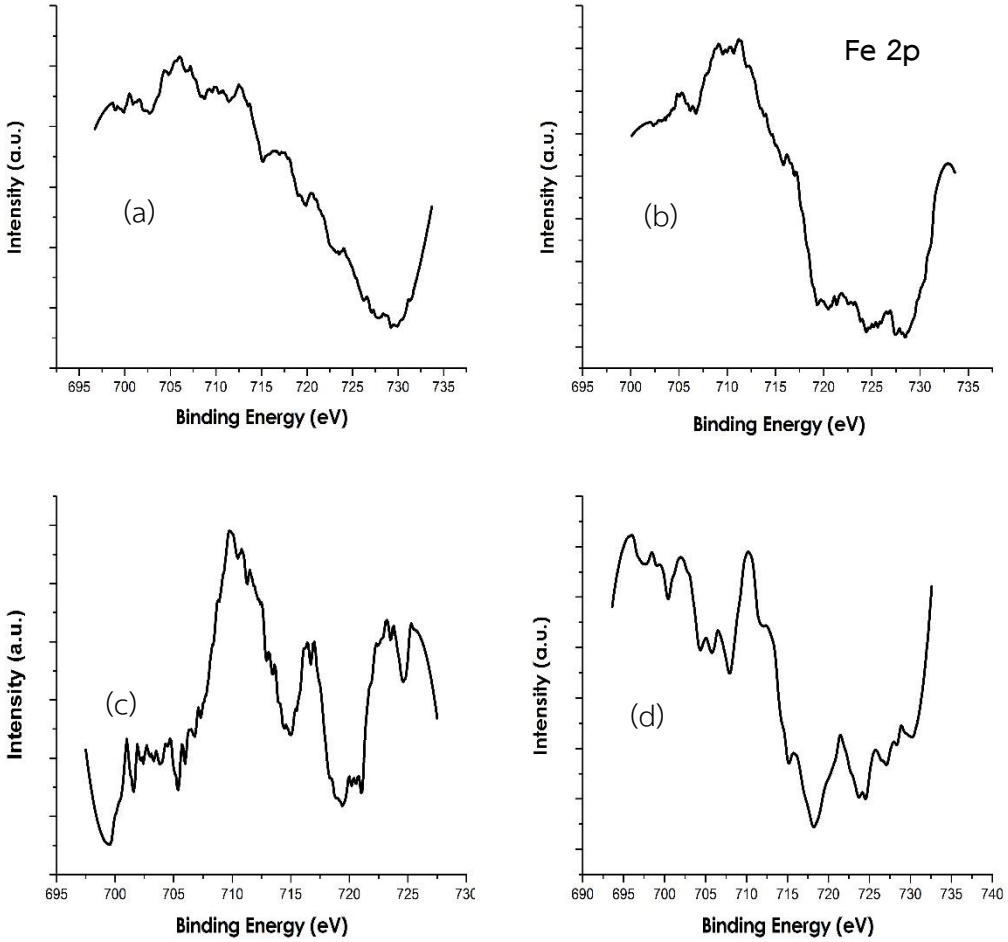

C.4 Fe XPS spectra of Fe 2p level for the 0.5Pt-xFe/TiO_2 series: (a) 0.5Pt-0.2Fe/TiO_2, (b) 0.5Pt-0.3Fe/TiO_2, (c) 0.5Pt-0.5Fe/TiO_2, and (d) 0.5Pt-0.7Fe/TiO_2

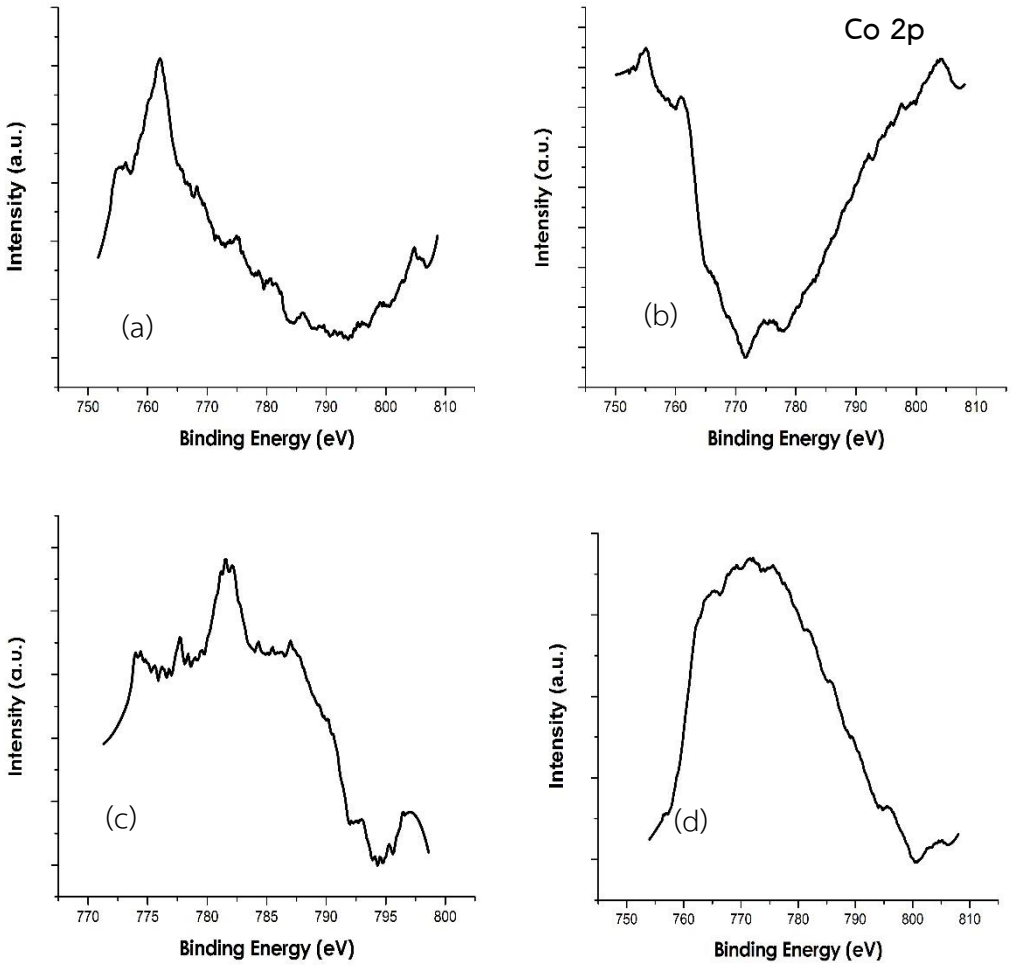

C.5 Co XPS spectra of Co 2p level for the 0.5Pt-xCo/TiO_2 series: (a) 0.5Pt-0.2Co/TiO_2, (b) 0.5Pt-0.3Co/TiO_2, (c) 0.5Pt-0.5Co/TiO_2, and (d) 0.5Pt-0.7Co/TiO_2

Appendix D

The TEM image of Pt based bimetallic catalysts and Pt monometallic catalyst

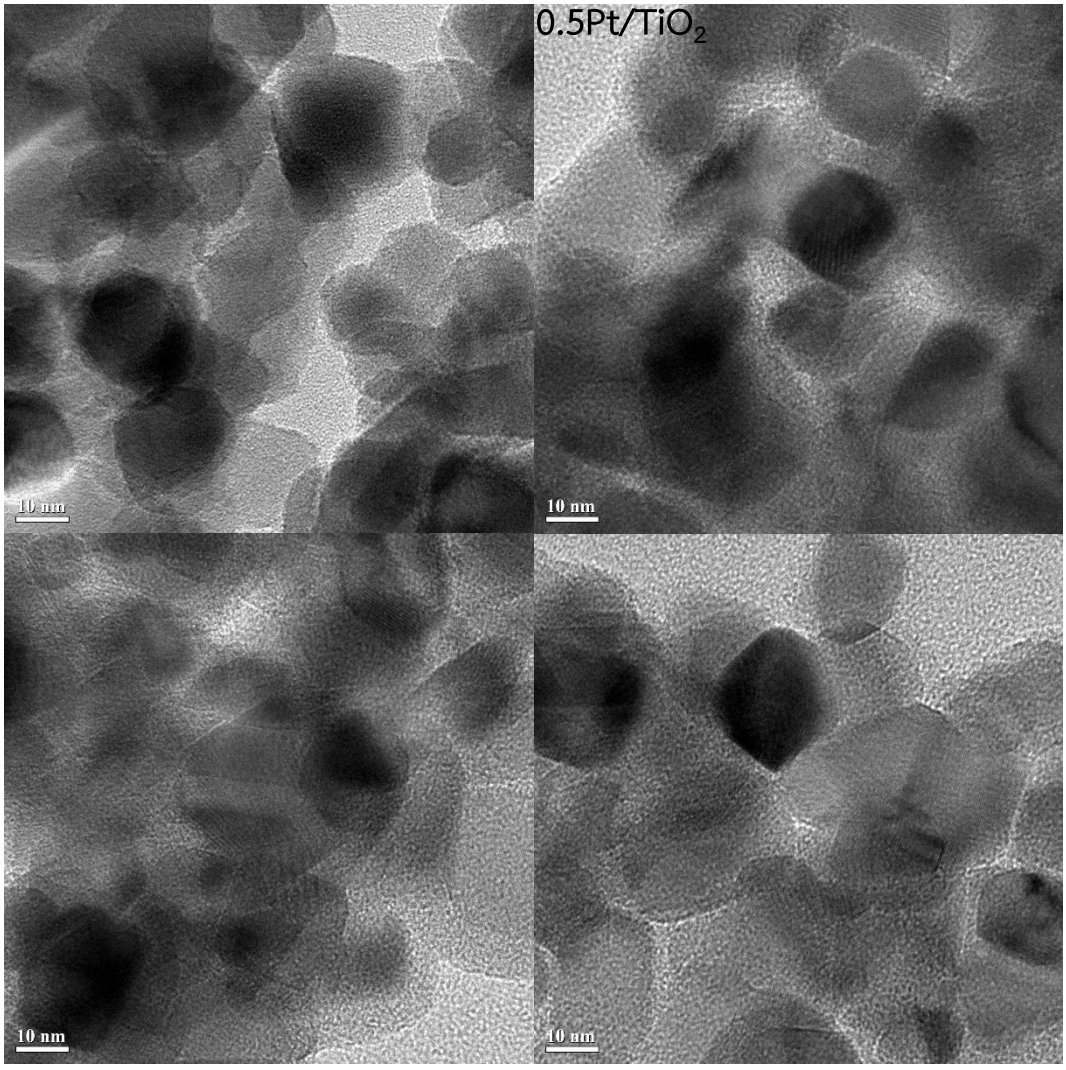

D.1 The TEM image of Pt monometallic catalyst

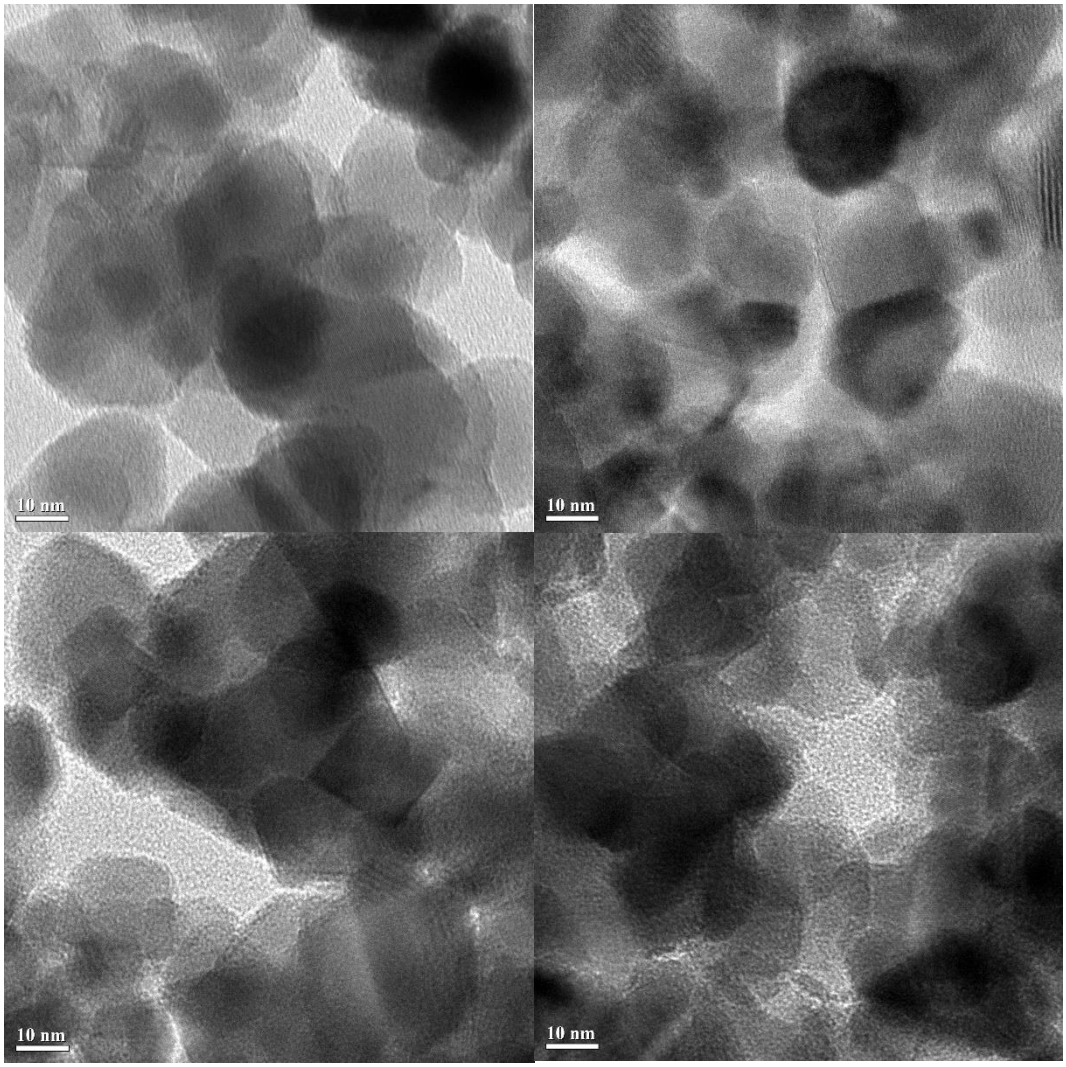

D.2 The TEM image of 0.5Pt-0.5Ga/TiO_2 catalyst

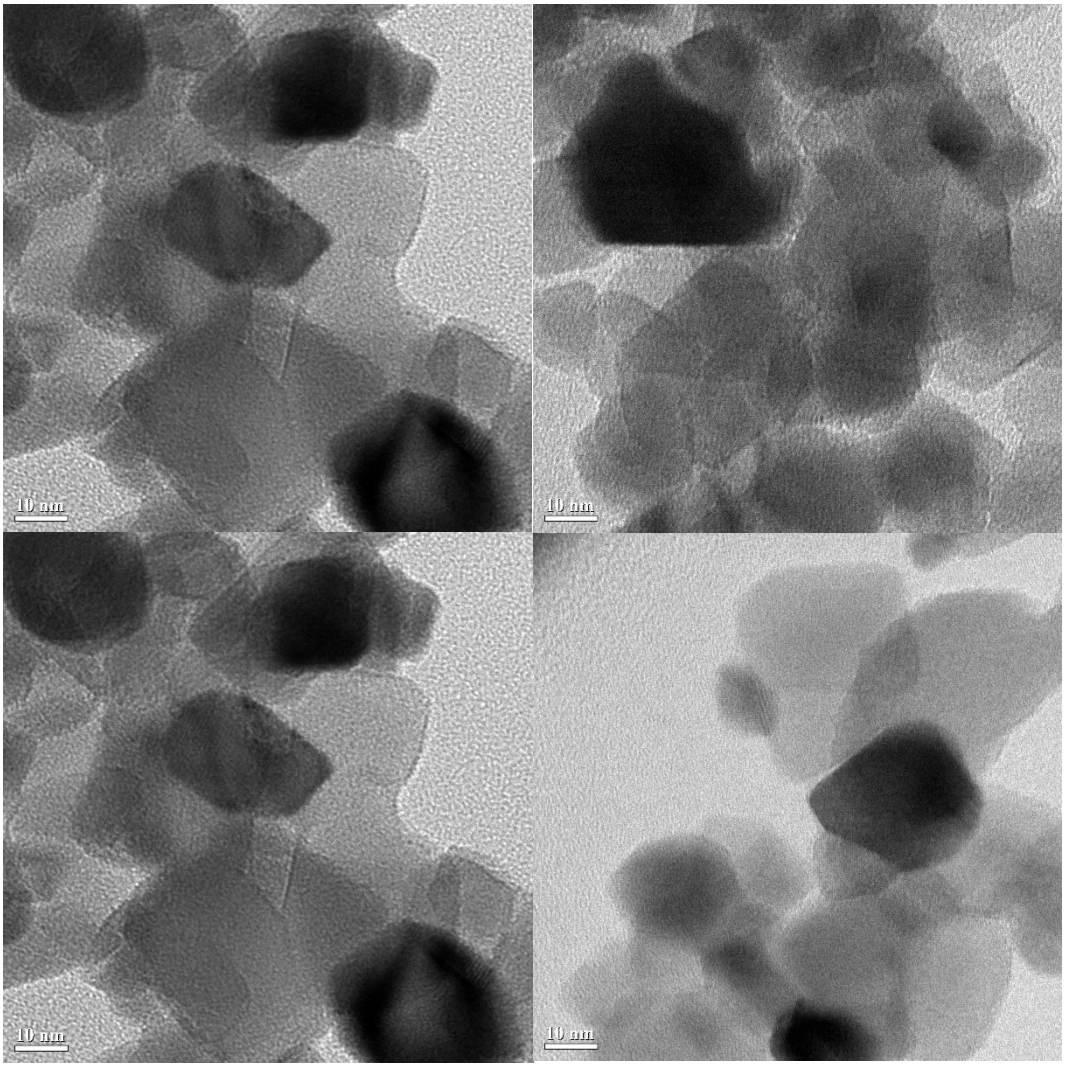

D.3 The TEM image of 0.5Pt-0.5Ni/TiO_2 catalyst

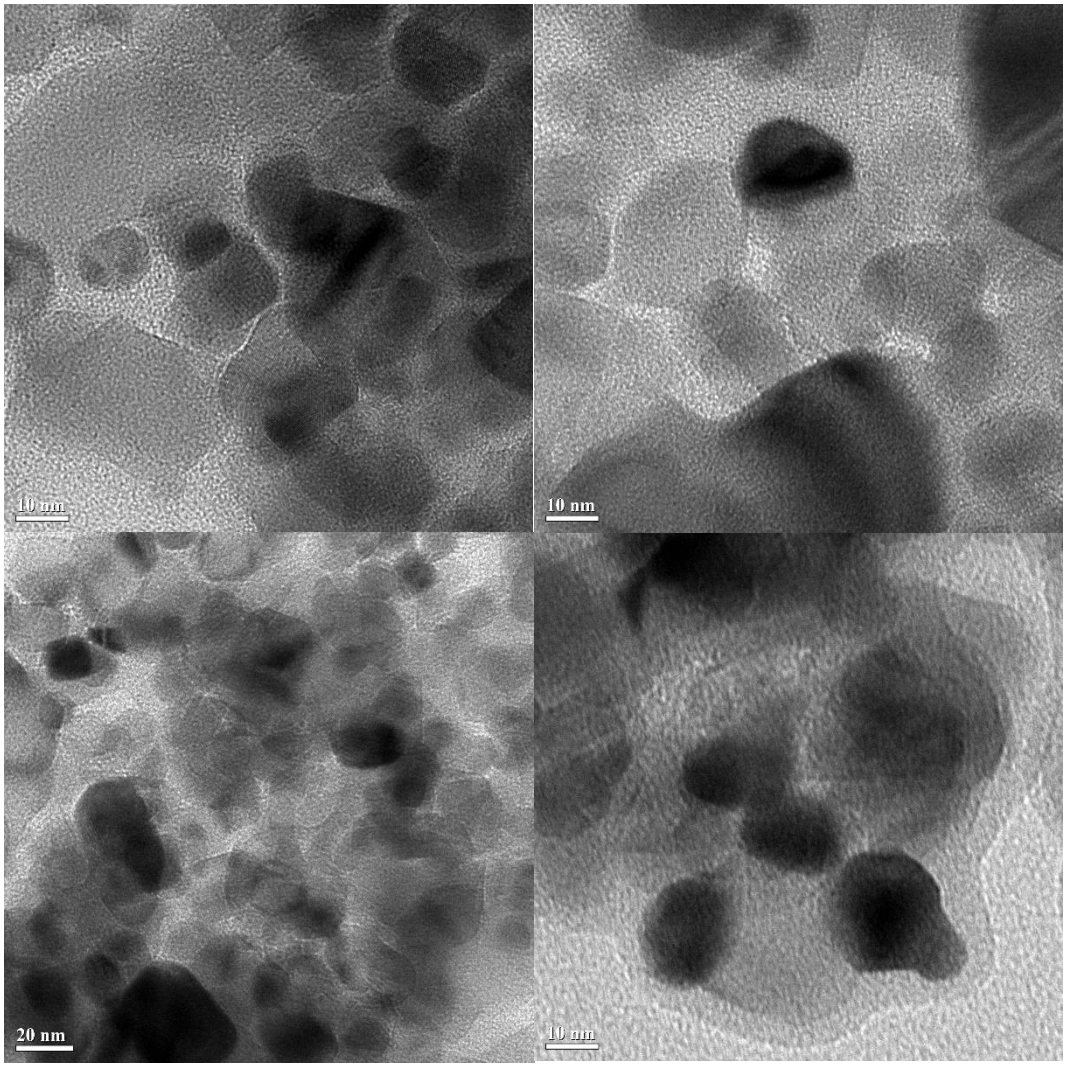

D.4 The TEM image of 0.5Pt-0.5Cr/TiO_2 catalyst

VITA

Mr. Sathaporn Tiensermsub was born on 28 September 1990, in Samutsongkarm, Thailand. He graduated Bachelor degree of Chemical Engineering from King Mongkut's University of Technology Thonburi, Thailand in May 2013. Since June 2013, he studied Master degree of Engineering from the department of Chemical Engineering, Chulalongkorn University.

The publication of research, SELECTIVE HYDROGENATION OF 3-NITROSTYRENE TO 3-VINYLANILINE OVER PT-BASED BIMETALLIC CATALYSTS was presented in The 4th Academic Conference on Natural Science for Young Scientists, Master & PhD Students from Asean Countries. 15-18 December, 2015 - Bangkok, Thailand by oral presentation and proceeding full paper at ISSN 978-604-913-088-5.